Motion thresholds can be predicted from contrast discrimination

Bettina L. Beard and Stanley A. Klein

School of Optometry, University of California, Berkeley, 360 Minor Hall, Berkeley, California 94720

Thom Carney

School of Optometry, University of California, Berkeley, 360 Minor Hall, Berkeley, California 94720; Neurometrics Institute, Oakland, California 94619

Received January 2, 1997; revised manuscript received April 1, 1997; accepted April 1, 1997

The detection thresholds for oscillatory motion and flicker were compared across a wide range of pedestal contrasts, spatial frequencies, and temporal frequencies in both foveal and peripheral vision. Motion and flicker stimuli were both generated by summation of a counterphase test grating with a static pedestal grating. For the oscillatory motion task the test and the pedestal were presented 90 deg out of phase to each other, whereas for flicker the two gratings were presented in phase. Since detection of both stimuli would depend on the same test stimulus, detection thresholds could be similar even though the tasks differ. Although there was a slight elevation in flicker detection thresholds compared with motion thresholds, our main finding is that oscillatory motion and flicker thresholds for suprathreshold sinusoidal gratings are similar. This finding supports the idea that motion and flicker have a common underlying detection mechanism. Our finding that flicker thresholds are slightly higher than jitter thresholds indicates that the contrast gain control (or saturating energy transducer) has a weak phase dependence. The ability to discriminate motion from flicker was elevated relative to their detection thresholds, particularly at high temporal frequencies. We offer two models to account for this behavior. The discrimination of motion from flicker may require a temporal comparison of the outputs of directionally selective filters tuned to opposite directions or to the population statistics of a bank of separable mechanisms. © 1997 Optical Society of America [S0740-3232(97)00809-0]

1. INTRODUCTION

Nakayama and Silverman[1] measured single-displacement motion thresholds for sinusoidal gratings and found that the phase angle required for seeing a displacement was inversely proportional to contrast for contrasts less than 2%. Above 2% contrast, however, phase angle thresholds were constant. These researchers suggested that the constant phase angle threshold could be explained if the effective contrast of the motion signal rapidly saturates with contrast. Their conclusion seems to differ from static contrast discrimination, where thresholds approximate Weber's law,[2,3] implying a logarithmic or power function increase in effective contrast, rather than a hard saturation. One of our goals in this paper is to investigate whether a common underlying mechanism can explain contrast effects for both motion and static contrast discrimination data. We use a test–pedestal paradigm to compare these seemingly dissimilar tasks.

Hu *et al.*[4] used a test–pedestal paradigm to compare vernier acuity and contrast discrimination for sinusoidal gratings. Under optimal conditions, the detection threshold for contrast discrimination (where the test stimulus is in phase with the pedestal stimulus) predicted the detection threshold for vernier acuity (where the test is in quadrature phase with the pedestal grating) when the two perceptually different stimuli were analyzed into the same test and pedestal components. This approach, which involves breaking down the stimulus into test and pedestal components and then plotting the data as a test threshold versus pedestal contrast (tvc) curve, is powerful since it requires no assumptions about spatial or temporal filter characteristics.[5] Typically, researchers use filter models to predict the fine position judgments of vernier acuity (e.g., Wilson[6]). A test–pedestal approach sidesteps filter model assumptions and, for optimal conditions, permits vernier acuity predictions based solely on contrast discrimination thresholds.[4,7–9] Thus a test–pedestal paradigm greatly simplifies some issues of vision research because it provides a method of comparing thresholds across different tasks.

In the present study we use a test–pedestal paradigm to empirically compare oscillatory motion with flickering contrast to determine whether the detection threshold for one task predicts the detection threshold for the other. We decompose oscillatory motion, or jitter, into a static pedestal grating and a superimposed counterphase test grating of the same spatial frequency presented in quadrature phase. Flicker is decomposed into these same test and pedestal gratings presented in phase to each other. The only difference between jitter and flicker is the phase relationship of the test and the pedestal. Since jitter and flicker detection thresholds depend on the visibility of the same test stimulus, similar detection thresholds would be predicted for the two tasks in the test–pedestal framework. The question of whether jitter

thresholds can predict flickering contrast thresholds is equivalent to asking whether contrast gain control depends on spatial phase.

Wesemann and Norcia[10] indirectly compared jitter and flicker thresholds. Figure 1 presents a tvc replot of their jitter data (open squares). Following their lead, we converted the Wright–Johnston[11] jitter thresholds (open circles) and the BodisWollner–Hendley[12] flicker thresholds (filled triangles) to contrast units. By comparison of the data in these different studies, it appears that the pedestal may be a more effective mask at slightly lower pedestal contrasts for flickering contrast than for jitter. We determine whether differences in the jitter and the flicker thresholds are due to the different experimental conditions and observers in the three studies. In our experiments we directly compare jitter and flicker in the same observers over a wide range of spatial and temporal frequencies.

A possible criticism of the test–pedestal approach is, How could it be otherwise? It seems apparent that motion and flicker thresholds would be similar if their detection depends on the visibility of the same test stimulus. Lawton and Tyler[13] found no difference in foveal thresholds for temporally ramped (250-ms total duration) or abrupt onset and offset (50-ms total duration) test gratings (1 and 7 c/deg) presented in phase and 90 deg out of phase with respect to a pedestal grating. Levi *et al.*,[8] however, found a breakdown in test–pedestal predictions in the periphery and in strabismic amblyopes, where they found a twofold to threefold elevation in vernier acuity thresholds relative to a comparable contrast discrimination task. Our data also show a violation of test–pedestal predictions under certain conditions. We sometimes (especially in the periphery) find a strong elevation in flicker compared with jitter thresholds. Thus the equality of jitter and flicker thresholds is not guaranteed. We examine these results and consider two models of how the visual system may process motion and contrast information in the fovea and in the periphery.

Similar temporal mechanisms have been proposed to account for detection of flicker and single-direction motion tasks.[14–19] Likewise, similar jitter and flicker detection thresholds for a broad range of parameters could signify that the same temporal mechanisms detect the two stimuli. However, similar thresholds for our jitter and flicker tasks could also result from different, independent mechanisms with similar sensitivities. We test whether the same mechanisms process jitter and flicker by also measuring their discrimination threshold. If both tasks use a purely transient mechanism that does not respond to the static pedestal, then thresholds for discriminating jitter from flicker should be elevated compared with jitter or flicker detection thresholds. Conversely, if discrimination is possible at the detection threshold, then different labeled lines may carry information about jitter and flicker.[20]

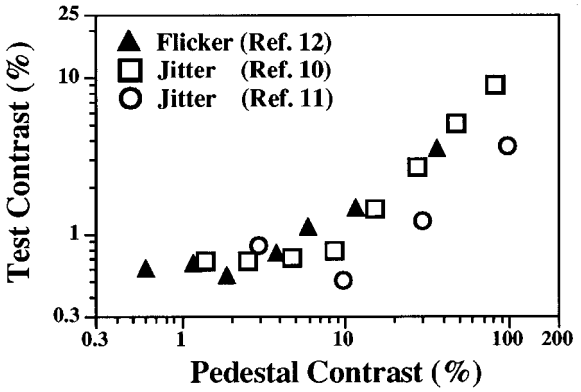

Fig. 1. Test contrast thresholds (%) as a function of pedestal contrast (%) for data from three studies. Replot (□) of jitter motion data from Wesemann and Norcia (observer HIW, Fig. 3, Ref. 10). Replot (○) of jitter motion data from Wright and Johnston (observer MW, Fig. 5, Ref. 11). Replot (▲) of counterphase flicker data from BodisWollner–Hendley (combined results of two observers at 6 c/deg, Fig. 2, Ref. 12).

Wright and Johnston[11] and Wesemann and Norcia[10] measured jitter thresholds in the periphery. Since there is a progressive reduction in cortical area devoted to a constant visual field region with increases in eccentricity, these investigators scaled the size of their peripheral stimuli.[21,22] Wesemann and Norcia[10] found a rightward shift and a reduced slope in the steady-rise Weber portion of the tvc curve, with increases in eccentricity. Because they did not obtain baseline counterphase flickering test detection thresholds (with zero pedestal contrast) at each eccentricity, it is unclear whether their scaling factor was adequate for temporally modulating gratings. We further explore these lower Weber fractions in peripheral vision to learn whether peripheral flicker detection and discrimination thresholds also reveal a rightward shift. Our results clarify whether the rightward shift is due to differences in detection with eccentricity or to the special role of motion in peripheral vision.

In the present research we had seven goals:

1. To extend measurements of the contrast dependence of jitter and flicker detection for foveal and peripheral vision to a wide range of spatial and temporal frequencies.
2. To determine whether the contrast gain control is phase dependent by comparing jitter and flicker thresholds by means of a within-subjects design for high, as well as low, pedestal strengths.
3. To determine the pedestal contrast at which detection thresholds begin to increase.
4. To determine whether motion and flicker are processed in the same temporal channels by comparing the contrast dependence of motion and flicker visibility with thresholds for discriminating between them.
5. To determine whether the cortical magnification scaling factor often used to equate static foveal and peripheral detection thresholds holds at high temporal frequencies. Is the rightward shift in the motion tvc curve with increased eccentricity[10] due to the use of an erroneous peripheral scaling factor, or is it due to distinct motion processing in peripheral vision?
6. To compare our oscillating grating results with the Nakayama–Silverman[1] single-displacement results. Do the data imply motion mechanisms that are saturating?
7. To develop a novel contrast discrimination dipper function fit for conditions in which the test and the pedestal stimuli are not the same.

2. METHODS

A. Apparatus and Stimuli

Horizontal sine-wave gratings were generated by a Neuroscientific VENUS stimulus generator and presented on a Tektronix 608 oscilloscope with P31 phosphor. The frame rate was 270 Hz. The display had a constant mean luminance of 120 cd/m^2 and was viewed from either 0.5 or 4.0 m through a rectangular aperture that subtended 7.6 deg × 11.9 deg visual angle from 0.5 m. We used a United Detector Technology photometer to calibrate luminance and contrast, and we maintained normal room illumination during each experimental session. A lookup table compensated for the ambient light that was present during the experiment. A surrounding visor prevented room lights from reflecting off the display.

Each 2-s presentation interval contained two superimposed sine-wave gratings: a visible static pedestal and a threshold counterphase flickering test. Figure 2 presents equations and phasor plots of the jitter and the flicker stimuli used in this study. Arrow lengths represent the pedestal (c_p) and the test (c_t) stimulus contrasts. The test and the pedestal always had the same spatial frequency. Jitter, produced by presentation of the test stimulus 90 deg out of phase to the pedestal grating, appeared as a smooth up-and-down displacement of the pedestal grating. Figure 2(a) represents this smooth displacement.[23] Figure 2(b) represents the flicker stimulus in which the test is an in-phase change in the contrast of the pedestal grating. The flicker stimulus appeared as a smooth, pulsating modulation of the pedestal contrast. The only physical difference between the jittering motion and the flickering contrast stimuli was the spatial phase relationship between the test and the pedestal components (0 deg for flicker and 90 deg for jitter).

A Gaussian temporal envelope ($\sigma = 0.33$ s) defined the onset and the offset of the test and the pedestal gratings, except in the 2-Hz condition. In the 2-Hz condition, we used abrupt stimulus onset and offset to obtain sufficient cycles in the 2-s exposure. In addition, two observers (SAK and TC) used abrupt stimulus onsets and offsets at several temporal frequencies other than 2 Hz to confirm that an abrupt onset cannot account for the elevated flicker-to-jitter ratio found at low temporal frequencies. Pedestal contrast ranged from 2% to 80%, test temporal frequencies ranged from 2 to 40 Hz, and test and pedestal spatial frequencies ranged from 0.5 to 20.0 c/deg.

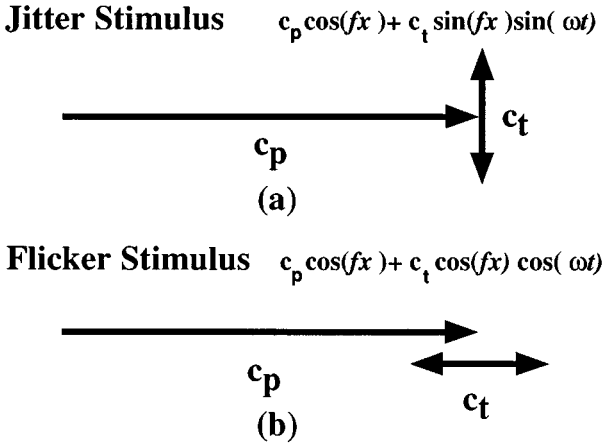

Fig. 2. Jitter and flicker stimuli used in the current experiments. (a) The jitter motion stimulus was composed of a counterphase test stimulus presented in quadrature phase compared with the pedestal stimulus. (b) The flicker consisted of a temporal increment in contrast. In the two equations, the pedestal and the test contrasts are given by c_p and c_t, respectively. Jitter and flicker stimuli differed only in the phase relationship of the pedestal and the test components.

B. Procedure

1. Jitter and Flicker Detection Thresholds

We obtained jitter and flicker detection thresholds by using a four-choice rating scale. The test stimulus contrast was randomly 0.0, 1.0, 1.5, or 2.0 times a base level that was close to each observer's threshold determined from pilot data. Observers practiced the task for approximately 10 trials before each block of 50–120 trials. We used unconstrained fixation, and the magnitude of the test grating was judged with a four-level rating after each trial. We also determined detection thresholds for the test stimulus without a pedestal at each spatial and temporal frequency, using the four-level rating scale.

2. Discrimination Thresholds

In the discrimination task, the observer determined whether the test stimulus was presented in phase (flicker) or out of phase (jitter) with the pedestal grating (a two-choice rating scale). The test contrast was the same for both phases.

Figure 3 shows a representation of the detection and the discrimination tasks in a two-dimensional signal detection response space.[24] The three large dots represent the three stimuli used in our experiments: The pedestal dot corresponds to the blank distribution in a signal detection experiment; the jitter and the flicker dots correspond to the signal distributions. The strength of the detection information is shown by the length of the diagonal lines, and the strength of the discrimination information is shown by the horizontal separation of the two signal distributions. In this figure discrimination is possible at the detection threshold, since discrimination and detection vector lengths are similar (a large angle between the jitter and the flicker vectors).

3. Periphery

For judgments in the periphery, observers fixated monocularly 17.5 deg eccentrically in the temporal field of the right eye. Since the visual system has reduced sensitivity to high spatial frequencies as eccentricity increases, test and pedestal spatial frequencies were low (0.5, 1.0, or 2.0 c/deg for observer PAS, and 0.5 c/deg for observers SAK, TC, QP, and BLB) when viewed from 0.5 m. Observer SAK (a presbyope) wore special correction for the near-viewing distance used in this study.

The 0.5-c/deg spatial frequency, at an eccentricity of 17.5 deg, is comparable in cortical size with a 4.0-c/deg foveal grating according to the scaling factor:

$$P(E) = P(0)/(1 + E/2.5), \quad (1)$$

where E is the eccentricity in degrees and $P(E)$ is the value of either spatial frequency or viewing distance at eccentricity E.[21,22] This is the same scaling factor used by

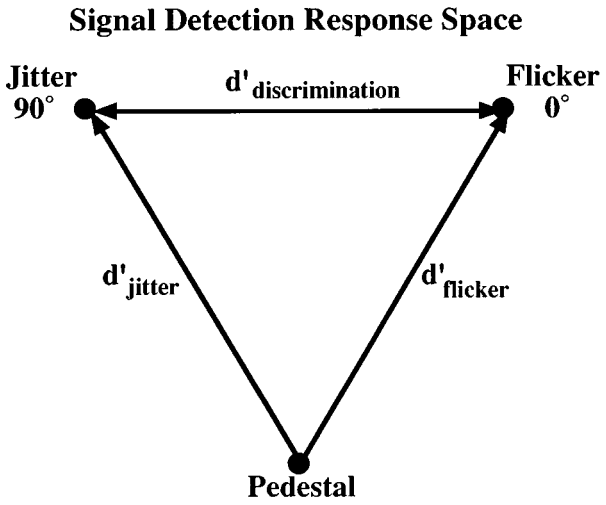

Fig. 3. Signal detection response space for the detection and discrimination tasks. Vector length determines the detection threshold. Our approach suggests that the detection vectors are similar for jitter and flicker. Discrimination is determined by the length of the difference vector. Here the discrimination threshold increases with increases in the detection threshold, since the discrimination vector length is the same length as detection.

Wesemann and Norcia,[10] who found a rightward shift in the tvc curve with eccentricity. We wished to determine whether this rightward shift was due to visibility differences for the eccentric conditions for two reasons. First, Wesemann and Norcia[10] did not report test detection thresholds without the pedestal. Second, we do not know whether the scaling factor that equates peripheral contrast sensitivity and grating resolution is the same for all temporal frequencies.

All the data collected within a session were fixed at one spatial and temporal frequency. Between blocks of trials, we varied the pedestal contrast and the stimulus type, either jitter and flicker detection or discrimination. Therefore learning effects should not account for differences between these measures. Auditory feedback after each trial indicated the actual stimulus level. Reported thresholds are those obtained after sufficient practice to reach a stable level of performance. Each reported threshold reflects 150–360 trials.

C. Data Analysis

We used the ROCFLEX signal detection program to estimate contrast threshold.[25] ROCFLEX uses a maximum-likelihood estimate of d' values for each stimulus and constructs a psychometric function relating d' to test stimulus contrast. We obtained three detection threshold estimates from the transducer functions: (a) when the transducer exponent was fixed at 1.5, (b) when it was fixed at 2.0, and (c) when it was unconstrained. Typically, the unconstrained exponent was between 1.5 and 2.0. Reported detection thresholds are based on the fixed slope threshold closest to the threshold calculated with an unconstrained slope. This procedure reduced variability because of outlier exponents. In the discrimination task we used a single contrast for both stimulus types; therefore the variable exponent transducer function fit was not possible. Reported discrimination thresholds are those obtained with a fixed exponent of 2.0. Plotted values are the geometric mean of at least three of these fixed slope thresholds weighted by the inverse variance of each datum.[26]

D. Observers

We tested seven observers with normal vision in various phases of the study. Observers AD, SAK, and QP viewed the display binocularly for foveal, and monocularly for peripheral, presentations. Observers TC, PAS, DJS, and BLB always viewed the display monocularly. All the observers had normal or corrected-to-normal visual acuity.

3. RESULTS

A. Visibility of Motion

Figure 4 presents foveal and peripheral contrast detection thresholds (T_d) for a counterphase flickering test grating (zero pedestal). Detection thresholds for two observers are shown: BLB (upper panel), and PAS (lower panel).

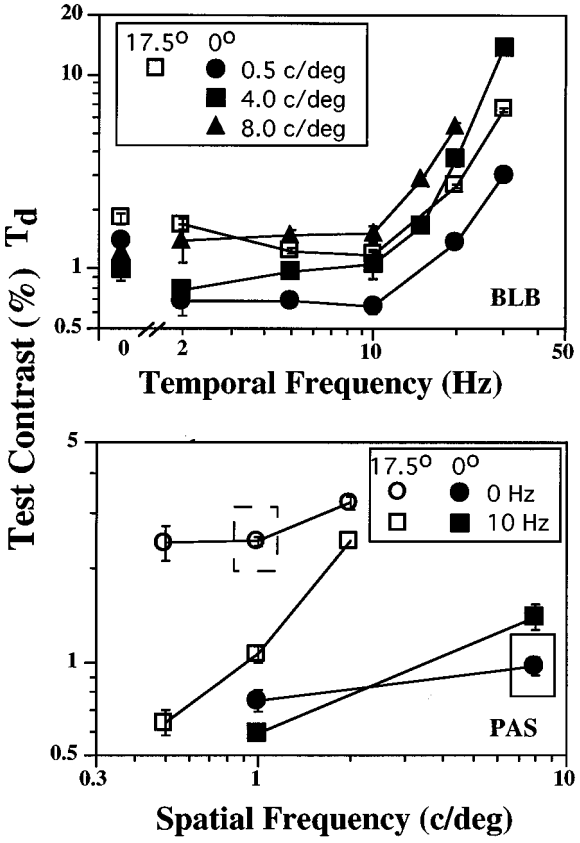

Fig. 4. Contrast detection thresholds for a counterphase test stimulus presented at different spatial and temporal frequencies for two observers. Thresholds for observer BLB are presented in the upper panel as a function of temporal frequency. Spatial frequency is represented by different symbols (●, 0.5 c/deg; ■, 4.0 c/deg; and ▲, 8.0 c/deg; □, 0.5 c/deg in the periphery). The lower panel shows thresholds for observer PAS as a function of spatial frequency. Data for different temporal frequencies are shown with separate symbols (●, 0 Hz and ■, 10 Hz for foveal data; ○, 0 Hz and □, 10 Hz in the periphery).

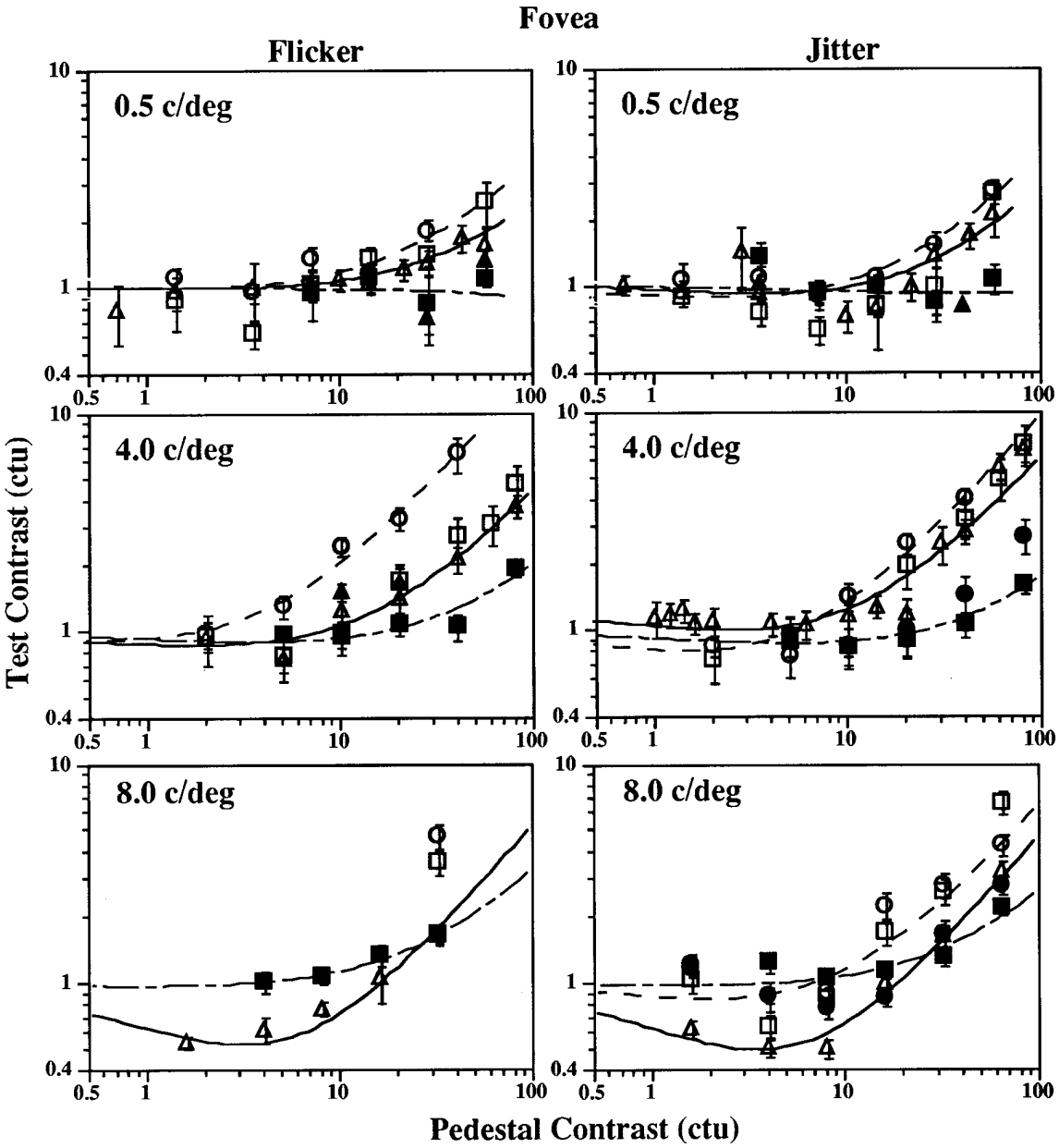

Fig. 5. Normalized test contrast thresholds as a function of normalized pedestal contrast for foveal viewing in observer BLB. A different spatial frequency is shown in each panel. Test stimulus temporal frequency is shown with different symbols (○, 2 Hz; □, 5 Hz; △, 10 Hz; ●, 15 Hz; ■, 20 Hz; ▲, 30 Hz). Flicker detection data are shown on the left; jitter, on the right. Fitted curves have been drawn through the 2-Hz (dashed curve), the 10-Hz (solid curve), and the 20-Hz (dotted–dashed curve) data.

First look at the detection data for BLB. We have plotted foveal and peripheral T_d as a function of temporal frequency at spatial frequencies of 0.5 c/deg (filled circles for foveal and open squares for peripheral), 4.0 c/deg (filled squares), and 8.0 c/deg (filled triangles). These contrast detection thresholds show the typical threshold increase at high temporal frequencies. A comparison of the 0.5-c/deg peripheral and foveal conditions (open squares and filled circles) reveals an elevation in the periphery compared with the fovea. However, there is little difference between the 4.0-c/deg foveal detection data and the scaled 0.5-c/deg peripheral data (filled versus open squares), particularly at higher temporal frequencies. It appears that the scaling factor used by Wesemann and Norcia[10] to equate foveal and peripheral temporal detection thresholds is adequate, since the 4.0-c/deg foveal and the 0.5-c/deg peripheral data are similar for this observer.

In the lower panel of Fig. 4 we show T_d as a function of spatial frequency at temporal frequencies of 0 Hz (circles) and 10 Hz (squares) for observer PAS. The filled symbols represent foveal data, and the open symbols represent peripheral data. PAS's peripheral 1.0-c/deg, 0-Hz data (enclosed in the dashed-line box) are elevated compared with the 8.0-c/deg, 0-Hz data (enclosed in the solid-line box), possibly because of peripheral adaptation effects.

B. Threshold Versus Pedestal Contrast Functions

We then fitted the raw (nonnormalized) jitter and flicker threshold data with the tvc curve:

$$c_t = \{[1 + (c_p/T_p)^n(1 + nw)]^{1/n} - c_p/T_p\}T_t. \quad (2)$$

This curve was derived from the transducer function discussed by Klein and Levi.[27] It represents a power function at low contrast and a logarithmic function at high contrast. We wanted to use a fitting function for the tvc curves based on a reasonable choice for the transducer function. For a derivation of this curve, see Appendix B. The free parameters for the fit are n, w, and T_t. The parameter n represents the low-contrast transducer exponent, w represents the contrast Weber fraction when contrasts are in contrast threshold units (ctu), and T_t is the fitted test threshold. The ratio c_p/T_p (pedestal contrast divided by the pedestal threshold) is the pedestal contrast in contrast threshold units. The fitting procedure, in the MATLAB nonlinear regression program, involved both the test and the pedestal contrasts in percent contrast. For the jitter and the flicker detection we always included the detection datum at zero pedestal contrast. If we had fitted normalized data, it would have been difficult to correctly weight the detection datum (zero pedestal). The detection datum was omitted from the fitting procedure for discrimination data, since discriminating jitter from flicker is meaningless without a pedestal. The fitting procedure minimized the chi square of the fit.

After curve fitting, we normalized the counterphase flickering test and static pedestal contrasts to their respective detection thresholds (T_d; see Fig. 4). Normalizing the data so that $d' = 1.0$ at threshold permits a comparison of temporal frequencies without the confounding effect of visibility differences. These normalized tvc curves are presented in Figs. 5–8. Thus both abscissa and ordinate are in contrast threshold units; i.e., the abscissa is the pedestal contrast divided by the pedestal detection threshold, and the ordinate is the test contrast divided by the test detection threshold, T_d. These figures show flicker detection (left-hand panels of Figs. 5 and 6), jitter detection (right-hand panels of Figs. 5 and 6), and the discrimination of jitter from flicker (Figs. 7 and 8) for observer BLB. Each panel shows the data for a different spatial frequency. Different symbols represent test stimulus temporal frequencies ranging from 2 to 30 Hz. Open symbols are used for lower temporal frequencies, filled symbols, for higher temporal frequencies (see caption for further details). Error bars represent ±1 standard error, calculated with the greater of the within-run and the between-run variances.[26]

The transducer fits are presented in Figs. 5–8 for the 2-Hz (dashed curve), 10-Hz (solid curve), and 20-Hz (dotted–dashed curve) conditions. Note that, as the pedestal contrast approaches zero, the fit is close to, but not exactly, unity. At zero pedestal contrast, the test contrast is given by the parameter T_t. This parameter is close to unity, since the main datum that constrains T_t is the detection threshold of the test pattern. Thus the intercept is T_t/T_d, where T_d is the measured detection threshold for the counterphase flickering test grating (Fig. 4). The fit with nonnormalized data will pass close to the detection threshold. It differs from the detection threshold because it is also dependent on low pedestal contrast thresholds.

The parameter n, in Eq. (2), represents the low-contrast transducer exponent. Its reciprocal describes the amount of facilitation seen in test thresholds. If $n = 1$, the system would be linear with no facilitation. A value of $n = 2$ would indicate the standard amount of facilitation that is found when the test and the pedestal are the same patterns. Klein and Levi[27] used $n = 2$ because their test and pedestal stimuli had the same spatial and temporal frequency. Here n is a free parameter for jitter and flicker detection, since the pedestal is a stationary grating and the test is a counterphase flickering grating of various temporal frequencies. One might expect that at low test temporal frequencies, where the test pattern becomes similar to the pedestal, the parameter n would approach 2, whereas at higher test temporal frequencies there would be little facilitation ($n = 1$), since greatest facilitation is typically seen for similar test and pedestal stimuli. For the discrimination of flicker from jitter, the transducer exponent was fixed at 1.1, close to the average of the flicker and jitter detection data. We could not permit n to float when fitting the discrimination data, since

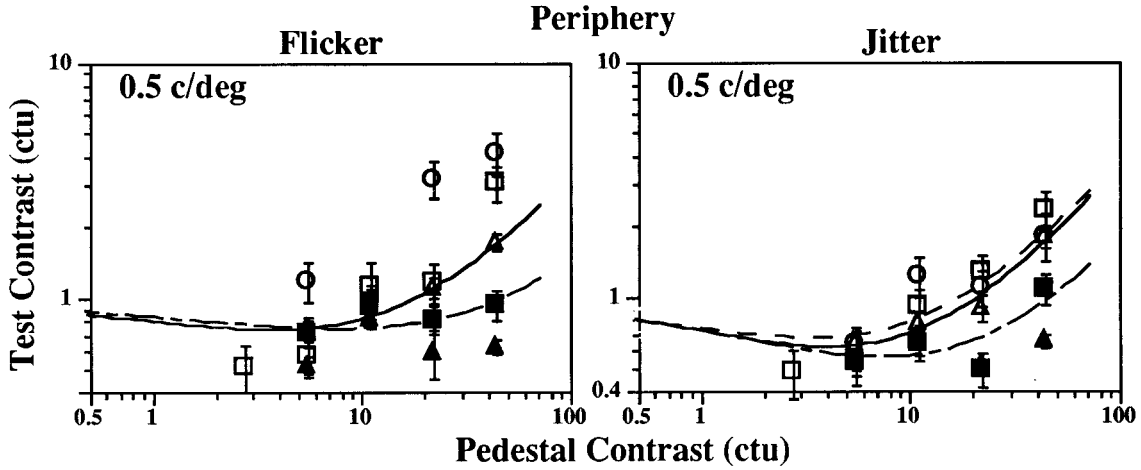

Fig. 6. Normalized test contrast thresholds as a function of normalized pedestal contrast for peripheral viewing in observer BLB. Symbols are the same as in Fig. 5.

the detection datum (zero pedestal) was not included in the fit.

In Figs. 7 and 8 the discrimination data at the highest temporal frequencies tend to have an elevated but shallow tvc curve. For this reason we did not fit these data with the tvc function with unity asymptotic slope. The summary data in Figs. 12 and 13 below for observer BLB (open circles) also show a plateau in that the discrimination is good at 40% contrast for the highest temporal frequencies.

Figures 9 and 10 (left-hand panels) presents these transducer exponents derived from the fits shown in Figs. 5–8 for jitter (squares) and flicker (circles) thresholds as a function of temporal frequency. Each panel shows the data for a different spatial frequency. Figure 9 shows foveal transducer exponents, while Fig. 10 shows exponents based on data collected at 17.5 deg eccentricity. The values of n, the transducer exponent, tend to be between 1 and 1.4. In general, for both fovea and periphery, the amount of facilitation is similar for jitter and flicker across stimulus conditions. Our expectation that n would be above 1.5 at low temporal frequencies was not verified. There is a tendency for jitter to show slightly more facilitation than flicker in the fovea, particularly at 5 Hz in the 4.0-c/deg condition.

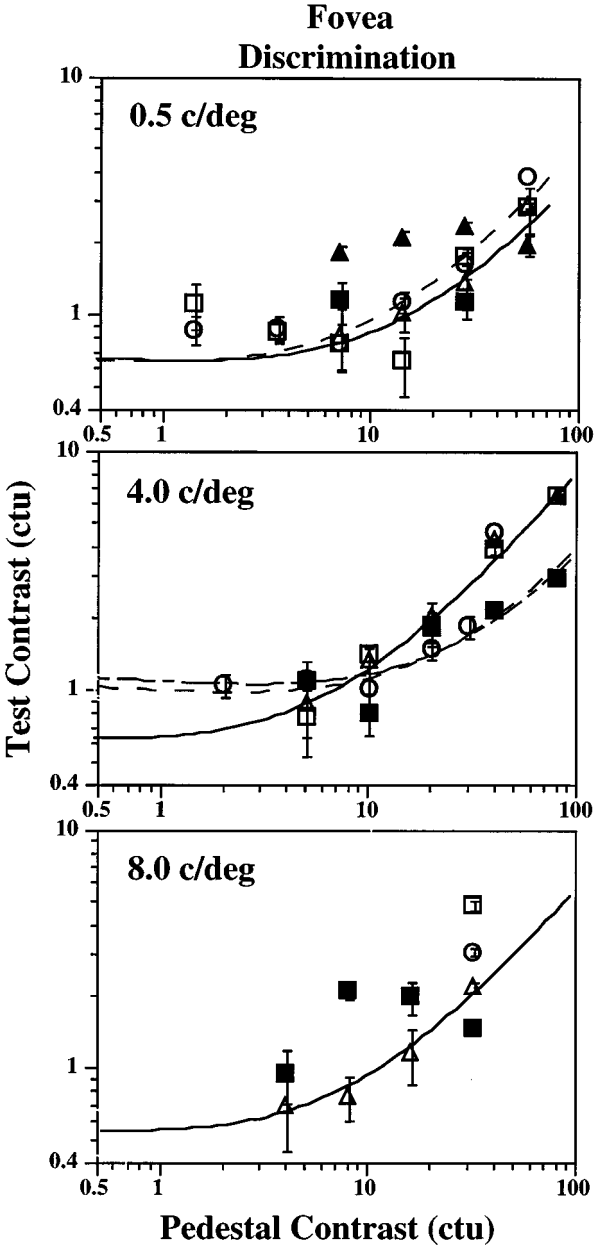

Fig. 7. Normalized test contrast thresholds as a function of normalized pedestal contrast for foveal viewing for the flicker/jitter discrimination task. Symbols are the same as in Fig. 5.

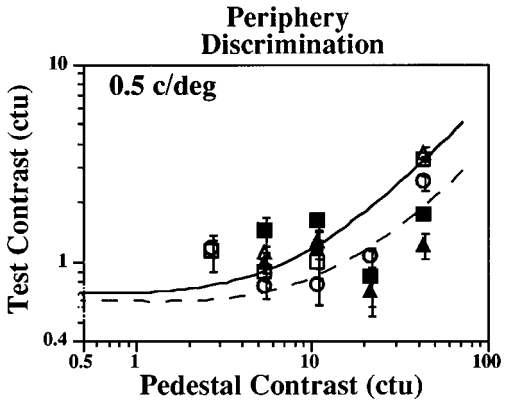

Fig. 8. Normalized test contrast thresholds as a function of normalized pedestal contrast for peripheral viewing for the flicker/jitter discrimination task. Symbols are the same as in Fig. 5.

The right-hand side of Figs. 9 and 10 presents w, the Weber fraction from the fitting functions shown in Figs. 5–8. Contrast Weber fractions are found to lie between 0.01 and 0.10 for temporal frequencies below 10 Hz and to decrease sharply for higher frequencies. In the fovea, Weber fractions are similar for jitter and flicker detection and for their discrimination, decreasing as temporal frequency increases. The reduced Weber fractions at 20 and 30 Hz suggest little, if any, masking effects at these high temporal frequencies. The tvc curves of Figs. 5–8 show this reduced masking by a rightward shift in the curves for the higher-temporal-frequency conditions.

Transducer exponents and Weber fractions are plotted in Fig. 11 for a temporal frequency of 10 Hz as a function of stimulus spatial frequency for observer PAS. Foveal data are presented in the upper two panels and peripheral data in the lower two panels. We do not show the Weber fraction for the discrimination data in the periphery because PAS's discrimination data were elevated even at low pedestal contrasts. This had the effect of not permitting a reliable fit for the discrimination data. Portions of PAS's detection and discrimination data are shown in Figs. 12 and 13.

Figures 12 and 13 present a summary of much of the data for the seven observers. Figure 12 shows foveal data, and Fig. 13 shows peripheral data. Data collected with a pedestal contrast of 10% are presented on the left, and data for 40% pedestal contrast are shown on the right. Different symbols represent the data of different observers. Symbols surrounded by a square indicate conditions in which the stimulus had abrupt onset and offset. In the fovea, the 4.0-c/deg foveal data are shown by filled symbols, while open symbols represent the 8-c/deg data.

The flicker-to-jitter detection ratio for foveal vision (Fig. 12) is plotted as a function of temporal frequency in the upper two panels. There is a trend for flicker thresholds to be slightly elevated compared with jitter thresholds, particularly at low temporal frequencies. In the second row of panels we have plotted the ratio of the discrimination threshold to the lower of the jitter and flicker detection thresholds. One must be cautious in interpreting the detection to discrimination ratios in the low-frequency region, since, as just mentioned, detection thresholds for jitter and flicker are dissimilar at low temporal frequencies. Thus their discrimination could be based on their visibility difference. Note, however, that our observers reported using different perceptual strategies (up-and-down motion for jitter versus changing contrast for flicker) for making the discrimination judgment. The difference in jitter and flicker thresholds was minimal at frequencies of 5 Hz and above. These higher-temporal-frequency conditions therefore provide insights into whether discrimination and detection thresholds differ. Under the 10% pedestal conditions (left-hand panels) elevated discrimination thresholds would be ex-

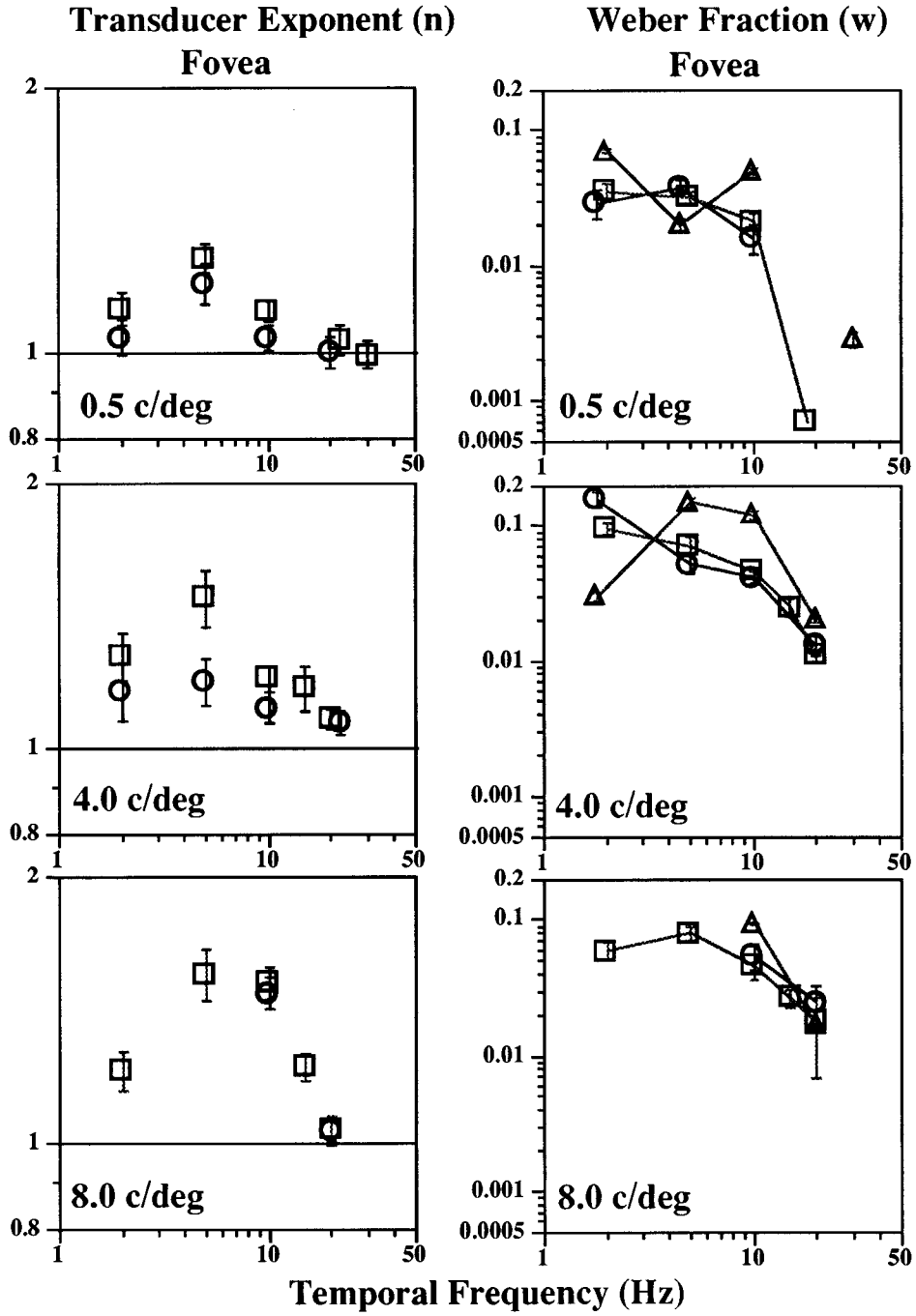

Fig. 9. Summary of the foveal data for flicker detection (○), jitter detection (□), and flicker/jitter discrimination (△) for observer BLB. Transducer exponents are plotted as a function of temporal frequency in the three left-hand panels, and Weber fractions are plotted as a function of temporal frequency in the three right-hand panels. Each panel presents the data for a different spatial frequency, as indicated.

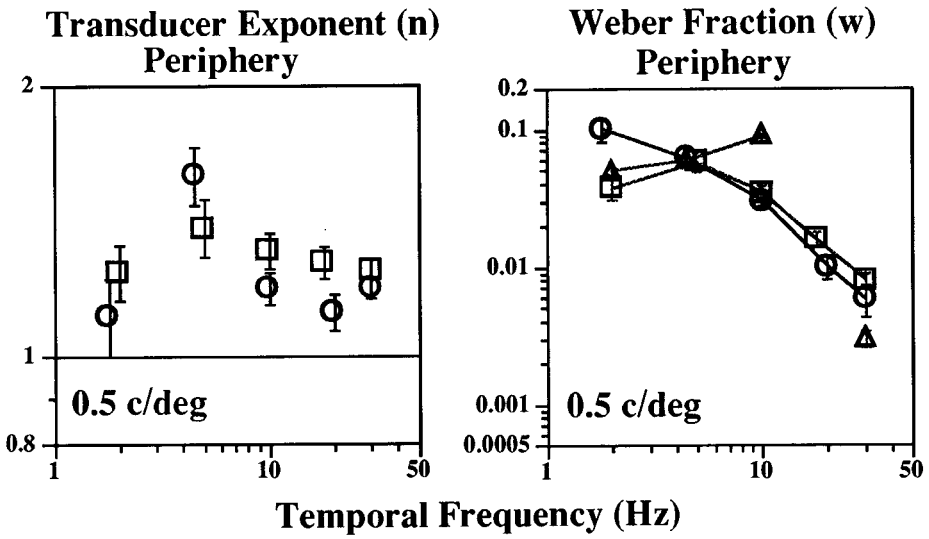

Fig. 10. Summary of the data for flicker detection (○), jitter detection (□), and flicker/jitter discrimination (△) in the periphery for observer BLB. The description is the same as in Fig. 9.

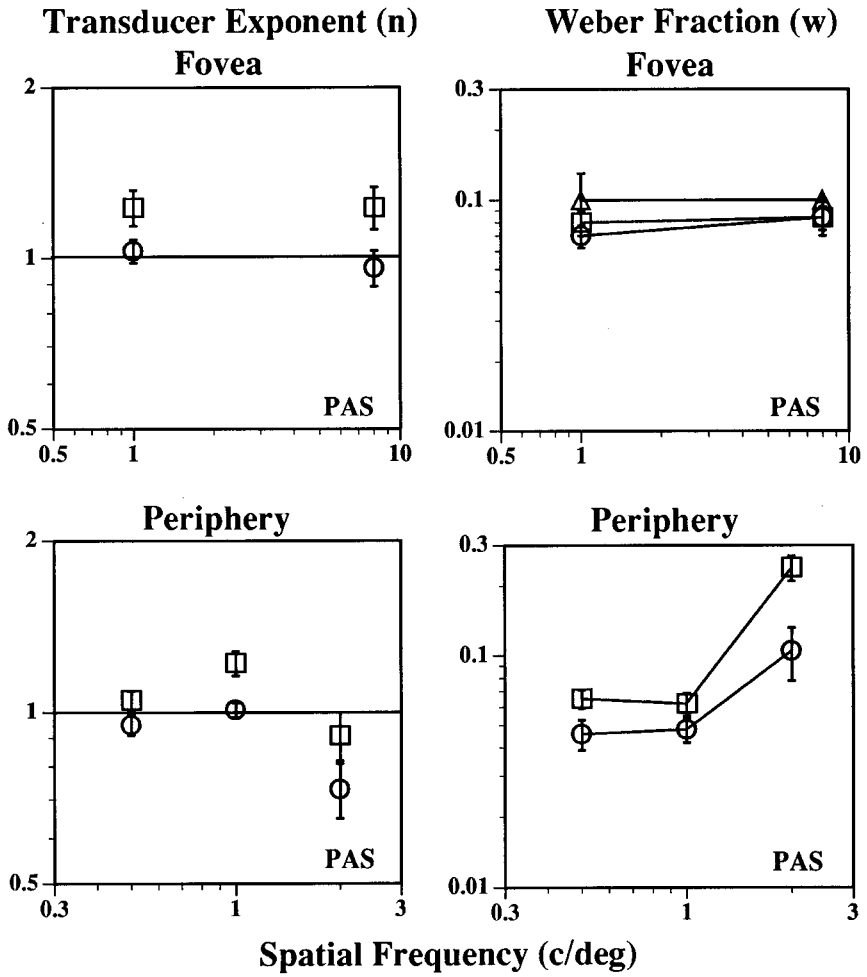

Fig. 11. Summary of the 10-Hz flicker detection (○), jitter detection (□), and discrimination (△) data at 8.0 c/deg in the fovea and 1.0 c/deg in the periphery for observer PAS. Low-contrast asymptotes and Weber fractions are presented as a function of spatial frequency.

pected, since discrimination is based on the visibility of the pedestal grating. Discrimination threshold elevation by as much as a factor of 2 at 40% pedestal (with many cases having the same jitter and flicker detection thresholds) suggests that similar mechanisms are responsible for jitter and flicker detection. If different mechanisms had been used, then discrimination should have been easier.

The four panels of Fig. 13 present flicker-to-jitter detection ratios and discrimination-to-detection ratios for data collected eccentrically. The conclusions are similar to those for foveal vision. Namely, flicker detection is consistently elevated by a small amount compared with jitter detection, particularly at low temporal frequencies. In addition, discrimination thresholds are elevated relative to detection at high temporal frequencies. We were surprised that the high-temporal-frequency jitter and flicker stimuli could be discriminated at any test contrast. We had anticipated that the test stimulus would be detected based on the counterphase flicker, with the pedestal being ignored, so that the ratio of discrimination to detection would be greater than the twofold to threefold loss that was obtained. Observers reported that they had a sense of the up-and-down motion of the jitter stimulus in the discrimination task even at 20 Hz and above.

Figure 14 presents the ratios of the jitter thresholds for 40% to the 10% pedestal contrast for foveal and peripheral conditions. In the Weber regime one would expect the ratio to be 4. Below 10 Hz, the ratios are close to the Weber regime in the fovea. In the periphery the ratios are approximately 2. This difference between the foveal and the peripheral detection threshold ratios suggests that the static 40% pedestal grating is not as effective in the periphery as it is in the fovea. The even lower ratios seen at high temporal frequencies represent little, or no, masking effects of the static pedestal on the flickering test grating visibility.

We calculated similar jitter detection ratios for the foveal and the 15-deg peripheral data of two observers in the Wesemann–Norcia[10] study (observers HIW and WFW in their Fig. 5). To compare with our 40% pedestal contrast, we averaged their 30% and 50% pedestal contrast thresholds and divided by their 10% threshold. For their two observers, these ratios are shown by star (★) symbols in Fig. 14. The similarity of their ratios to the present investigation's ratios shows that masking is similar in both studies. In the periphery, the static pedestal produces less masking than in the fovea. This lack of masking cannot be explained by raised peripheral thresholds, since Fig. 4 shows that, for BLB, the thresholds are not substantially different between fovea and periphery when our scaled stimuli are used. The insensitivity of the pe-

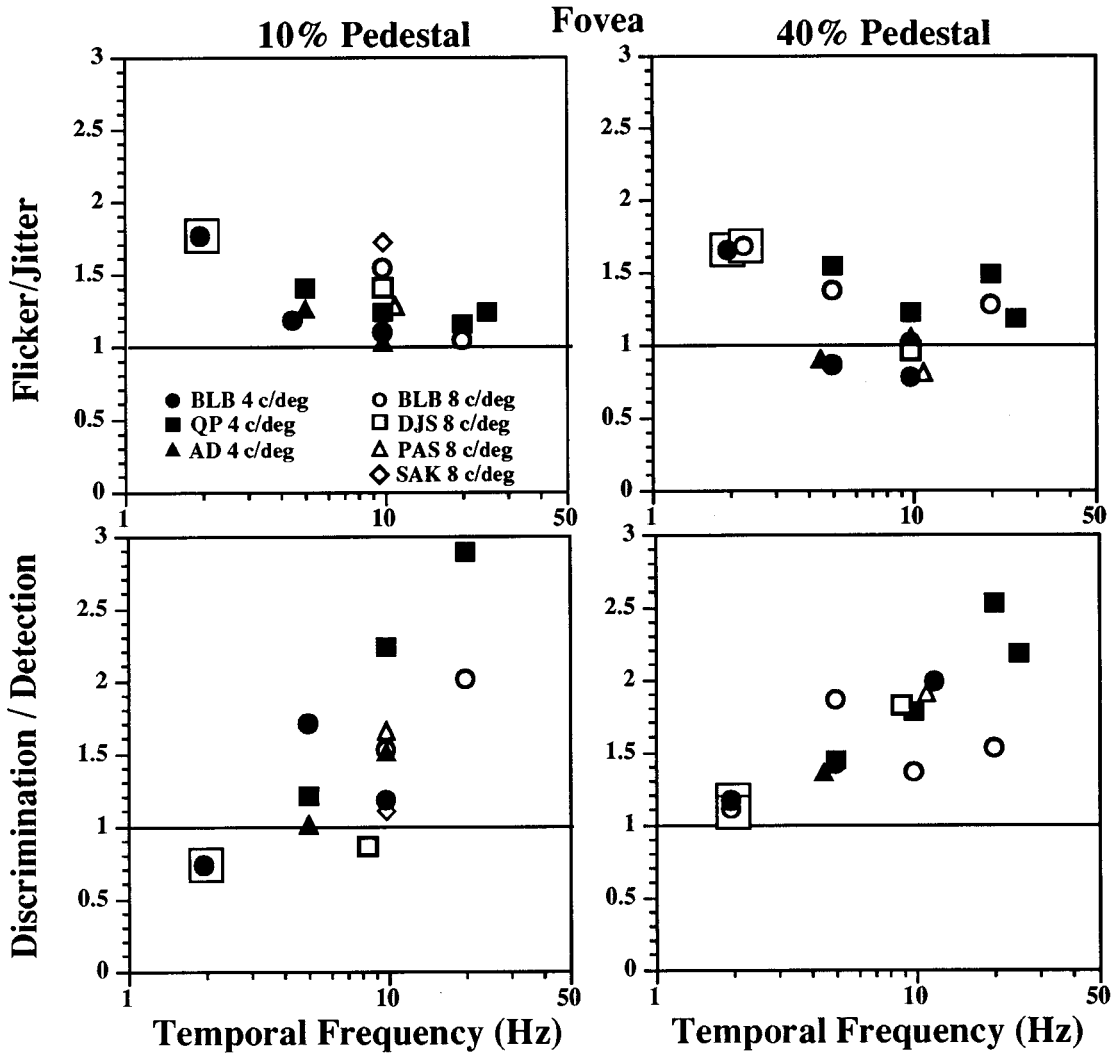

Fig. 12. Flicker/jitter and discrimination/detection ratios as a function of temporal frequency for the 4- and the 8-c /deg foveal data of all the observers. Each symbol represents a different observer. Data obtained with stimuli presented with a square wave onset and offset are enclosed in squares.

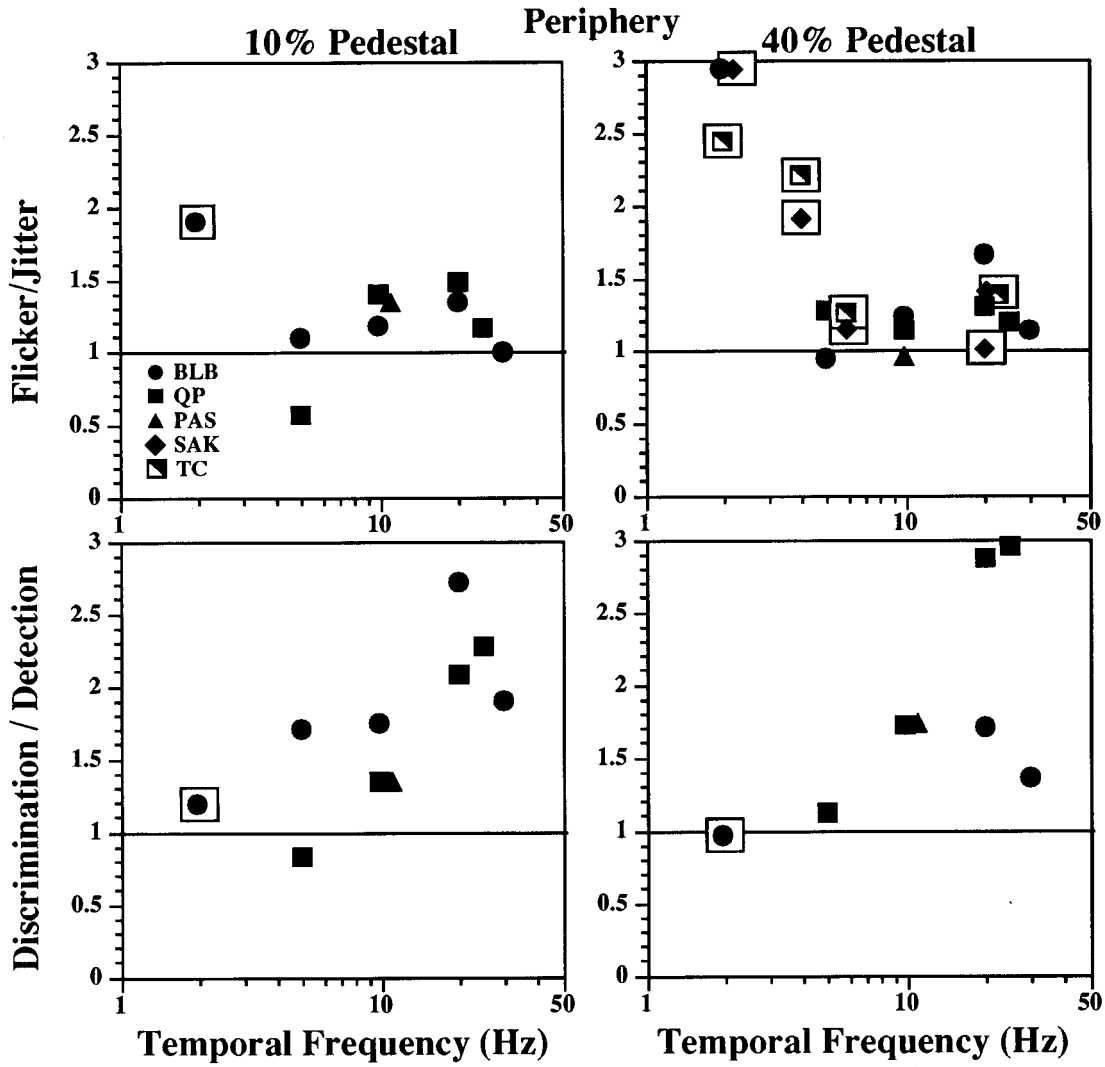

Fig. 13. Flicker/jitter and discrimination/detection ratios as a function of temporal frequency for the 0.5- and the 1.0-c/deg eccentric data of all the observers. The description is the same as in Fig. 12.

riphery to the pedestal probably can be seen best in Fig. 6, where the tvc curves are plotted in ctu that discount detection thresholds.

4. DISCUSSION

We measured detection thresholds for a flickering test grating presented either out of phase (jitter) or in phase (flicker) with a static pedestal grating. Our first goal in this paper was to determine the contrast dependence of jitter and flicker detection over a wide range of spatial and temporal frequencies in foveal and peripheral vision. The general findings (see Figs. 5–8) in both fovea and periphery were that contrast threshold remains around the unmasked threshold until the pedestal is approximately 10–20 ctu. Jitter and flicker thresholds show some facilitation at low pedestal contrasts (below 20 ctu), particularly when the test temporal frequency was 5 Hz. At higher pedestal contrasts (beyond 20 pedestal ctu), test thresholds rise steadily, with greater masking at the lower temporal frequencies. A likely explanation for the elevated thresholds seen at lower temporal frequencies is that under these conditions the test temporal characteristics are most similar to the static pedestal, and masking is greatest because both the test and the pedestal fall within the temporal receptive field of a single mechanism.

One of our subsidiary goals was to develop a data fitting framework for the case of masking when the pedestal and the test are different patterns. The fitting function must take into account the different thresholds of the test and the pedestal and must allow for the possibility of facilitation and of reduced masking. An analytic formula for a tvc curve that satisfies these conditions is derived in Appendix B and was presented in Eq. (2).

A. Summary of Related Test–Pedestal Experiments

Another goal in this paper was to determine limitations of the test–pedestal approach, since failures of the approach (jitter and flicker thresholds not being equal) are informative about the nature of the underlying mechanisms. We found that test–pedestal predictions fall short, since flicker thresholds were slightly higher than jitter detection thresholds (Figs. 12 and 13), particularly at low temporal frequencies. In this section we address successes

and failures of the approach in related experiments. By use of a range of tasks, the results in these experiments suggest that, under some conditions, the masking effects are slightly greater when test and pedestal components are added in phase.

We hypothesized that if two perceptually distinct stimuli can be decomposed into the same test and pedestal components (differing only by a phase shift), then the detection threshold for one may be used to predict the detection threshold for the other. We wondered whether the same prediction would hold if the test and the pedestal components were identical or differed in spatial or temporal frequency in addition to differing in their phase relationship. Table 1 provides a summary of this research. In each study (except Ref. 25, as discussed below) the pedestal, or the background, stimulus is a static cosine grating. The test grating either is identical to the pedestal or differs from the pedestal in spatial frequency, phase, or temporal frequency.

1. Present Study

In the present study the test stimulus was a counterphase flickering sine-wave grating of the same spatial frequency as a superimposed stationary pedestal grating. Rows 1 and 2 of Table 1 show the pedestal and test components for the jitter and the flicker detection conditions. As predicted, since both test stimuli differed only in the relative phase relationship of the components, we found similar detection thresholds in the fovea and the periphery for jitter and flicker, although flicker thresholds were slightly elevated compared with jitter detection thresholds. Thus flickering contrast does a reasonably good job of predicting the visibility of motion (jitter), supporting the test–pedestal approach for a wide range of spatial and temporal frequencies.

Row 3 of Table 1 shows the stimulus for our discrimination task. There was an elevation in discrimination thresholds compared with detection in foveal and peripheral vision as temporal frequency increased (see Figs. 12 and 13). Below we discuss the discrimination threshold results in the context of whether jitter and flicker are processed within the same or different mechanisms. The column labeled "Case" refers to three types of test–pedestal experiments that are discussed in Appendix A. The last two columns of Table 1, labeled "Facilitation" and "Masking" are discussed in Subsection 4.B.

2. Detection Versus Discrimination of Motion and Contrast

Our experiment involved sinusoidally oscillating position and contrast. Similar experiments have been performed with an abrupt change in position or contrast. Focusing on the experiment of Nakayama and Silverman,[1] row 4 of Table 1 presents their displacement detection stimulus and is written in a way that emphasizes the similarity between their single-displacement and our jitter experiments. The only difference between jitter detection (row 1) and the detection of a single displacement (row 4) is that the oscillating term, $\cos(\omega t)$, is replaced by the contrast reversal function, $R(t)$, where

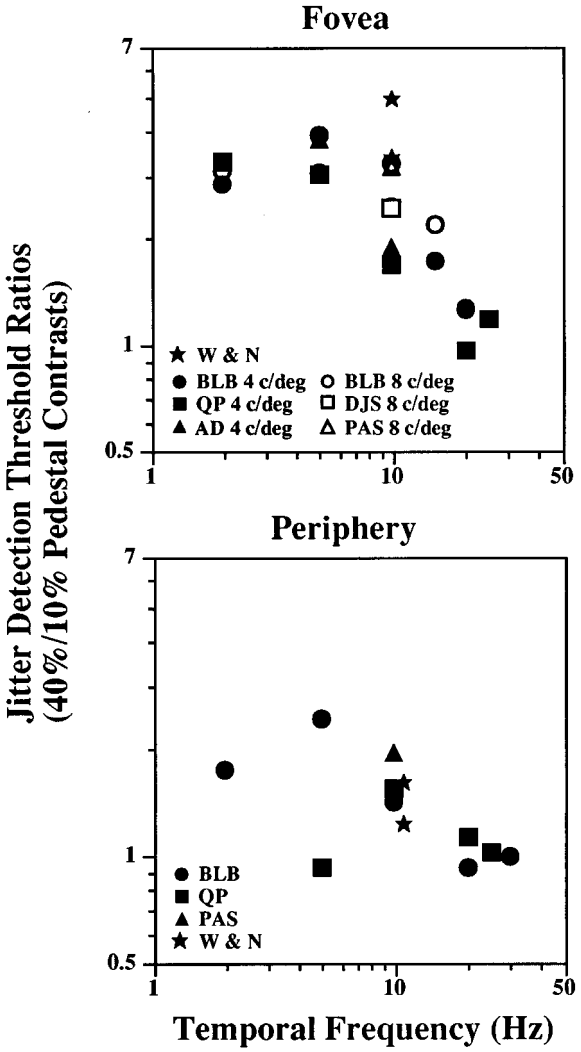

Fig. 14. Jitter detection threshold ratios between two pedestal contrasts as a function of test stimulus temporal frequency. Each symbol represents a different observer, as indicated in the legend. The starred (★) data are ratios calculated from two observers in the Wesemann–Norcia[10] study.

$$R(t) = +0.5 \quad \text{for } t > 0,$$
$$R(t) = -0.5 \quad \text{for } t < 0. \tag{3}$$

Thus, for $t > 0$, the stimulus is shifted rightward by one half the total displacement, and for $t < 0$ the stimulus is shifted leftward by the same amount. Detection of the displacement corresponds to discriminating the difference between a stimulus with no jump and a stimulus with a rightward jump. (The displacement detection task is case 2b of Appendix A and is shown as a phasor diagram in Fig. 20 below.) Besides measuring single-displacement detection thresholds, Nakayama and Silverman[1] measured direction discrimination thresholds,[34] using the same apparatus (refer to row 6 of Table 1). Rather than discriminating a jump from a no-jump condition (detection of displacement), the observer discriminated a rightward jump from a leftward jump (discrimination of direction). (This task is case 3 of Appendix A and is shown as a phasor diagram in Fig. 20 below.) Levi *et al.*[25] also measured detection and discrimination of single displacements; however, their stimuli

were composed of rectangular rather than sinusoidal gratings. They found that, while detection and discrimination thresholds were similar in foveal vision, in the periphery discrimination was degraded.

Row 5 of Table 1 presents the test–pedestal stimulus for contrast discrimination where there is an abrupt change in contrast rather than a change in phase. The Stromeyer–Klein[28] study is a good comparison with Nakayama and Silverman.[1] Both used a single interval with an interstimulus interval of 0, where the test grating was added to a continuously presented pedestal grating with no temporal gap. Nachmias and Sansbury[2] and Legge and Foley[3] presented two alternatives (pedestal versus pedestal plus test) that were separated by a temporal gap (interstimulus interval of 250 and 750 ms, respectively). The Lawton–Tyler[13] study compared a phase jump with a contrast jump, but instead of using a step for $R(t)$ they used either a 50-ms rectangular pulse or a 250-ms half-cosine pulse. They found overlapping tvc curves for in-phase and out-of-phase modulation.

3. Vernier Acuity Versus Contrast Discrimination

Hu *et al.*[4] examined test–pedestal predictions by comparing vernier thresholds with thresholds for a contrast increment on half the grating. A vernier stimulus can be decomposed into a stationary test grating presented out of phase to a stationary pedestal grating. The components of the Hu *et al.*[4] stimuli are shown in rows 8 and 9 of Table 1. The contrast increment and vernier tasks differed only in the phase relationship of the test and pedestal gratings. This is a 0-Hz version of the present experiments. Unlike the single field stimulus arrangement used in the present study, Hu *et al.*[4] used a split-screen display so that the observer could simultaneously compare the pedestal alone with the pedestal plus test stimulus. An abutting comparison was needed for the optimal vernier case (row 7), where a phase shift provided the detection cue. They found that under optimal conditions thresholds were similar for each task, so that contrast discrimination thresholds could be used to predict vernier acuity thresholds. There were a number of small, but important, differences in results between the two tasks. These subtle deviations are informative about the nature of the underlying mechanisms. For example, tvc curves for the vernier task showed no facilitation, and tvc slopes were slightly shallower for vernier. Thus at high pedestal contrasts a test pattern that was added with a 90-deg phase shift relative to the pedestal was slightly more vis-

Table 1. Summary of Research Shown within the Test–Pedestal Framework[a]

Task	Pedestal	Test	Case	Facilitation	Masking
Present study					
1. Detect jitter [b–d]	$\cos(fx)$	$\sin(fx)\sin(\omega t)$	1	yes at low hertz	hcm
2. Detect flicker[d,e]	$\cos(fx)$	$\cos(fx)\cos(\omega t)$	1	yes	hcm
3. Discriminate jitter and flicker[d]	$\cos(fx)$	$\cos(fx)\cos(\omega t)$	–	yes	foveal hcm
		$\sin(fx)\cos(\omega t)$			peripheral lcm, hcm
Detection and discrimination of displacement (single-jump version of present study)					
4. Detect single displacement[f–h]	$\cos(fx)$	$\sin(fx)\,R(t)$	2	yes	lcm
5. Detect contrast increment[h–k]	$\cos(fx)$	$\cos(fx)\,R(t)$	2	yes	lcm
6. Discriminate displacement direction[f,g]	$\cos(fx)$	$\pm\sin(fx)\,R(t)$	3	yes	lcm
Vernier (0-Hz version of present study)					
7. Detect vernier offset[l,m]	$\cos(fx)$	$\sin(fx)\,R(y)$	2		
8. Detect contrast increment[n]	$\cos(fx)$	$\cos(fx)\,R(y)$	2	yes	lcm
9. Discriminate vernier direction[l–n]	$\cos(fx)$	$\pm\sin(fx)\,R(y)$	3	no	slight
Frequency and amplitude modulation (spatial version of present study)					
10. Detect spatial structure (FM)[o]	$\cos(fx)$	$\sin(fx)\sin(f_m x)$	1		
11. Detect contrast increment (AM)[o]	$\cos(fx)$	$\cos(fx)\cos(f_m x)$	1		
Counterphase pedestal (identical test as in present study)					
12. Detect rightward motion [p,q]	$\cos(fx)\cos(\omega t)$	$\sin(fx)\ \sin(\omega t)$	–	yes	slight
13. Detect temporal contrast increment [p,q]	$\cos(fx)\cos(\omega t)$	$\cos(fx)\ \cos(\omega t)$	–	yes	

[a] f and ω are the spatial and temporal frequencies of the stimulus, respectively. $R(t)$ represents a temporal jump. Studies showing a high-contrast masking (hcm) kneepoint are distinguished from those showing low-contrast masking (lcm).
[b] Ref. 10 (Wesemann and Norcia).
[c] Ref. 11 (Wright and Johnston).
[d] Present study.
[e] Ref. 12 (BodisWollner and Hendley).
[f] Ref. 1 (Nakayama and Silverman).
[g] Ref. 25 (Levi *et al.*).
[h] Ref. 13 (Lawton and Tyler).
[i] Ref. 3 (Legge and Foley).
[j] Ref. 28 (Stromeyer and Klein).
[k] Ref. 2 (Nachmias and Sansbury).
[l] Ref. 29 (Bradley and Skottun).
[m] Ref. 30 (Funakawa).
[n] Ref. 4 (Hu *et al.*).
[o] Ref. 31 (Jamar *et al.*).
[p] Ref. 32 (Stromeyer *et al.*).
[q] Ref. 33 (Lubin).

ible than when added in phase. This result agrees with our results, in which jitter is slightly more visible than flicker. Hu *et al.*[4] did not carry out a discrimination task in which the observer had to discriminate between the stimuli in rows 7 and 8 (similar to the flicker-versus-jitter discrimination of row 3).

Rows 5 and 8 of Table 1 both present contrast increment detection studies. There are differences and similarities between these studies. In the row 5 studies, the test and the pedestal stimuli were superimposed spatially to match the single-displacement stimulus presented in row 4 of Table 1, whereas in the study shown in row 8 the test and the pedestal were presented side by side to match the vernier offset stimulus in row 7.

Another experiment that is similar in structure to our jitter and flicker experiment is that of Jamar *et al.*[31] They compared the detectability of quasi-spatial-frequency modulation (row 10) and amplitude modulation (row 11) in fovea and periphery. Amplitude, or contrast, modulation thresholds (the in-phase condition) were elevated compared with spatial-frequency modulation thresholds (the quadrature phase condition), in agreement with our temporal modulation results, although the elevation that they reported was much greater. They also found that information about suprathreshold contrast increments and phase is not as efficiently processed in the periphery, similar to our results for contrast increments (flicker). We did not find, as they did, that peripheral phase processing was worse, since our discrimination thresholds were similarly elevated in both fovea and periphery (Fig. 13).

4. Counterphase Pedestals

It is useful to mention a case in which the naïve application of the test–pedestal approach fails. Rows 12 and 13 in Table 1 present the pedestal and the test components used by Stromeyer *et al.*[32] and by Lubin.[33] In these studies a counterphase test stimulus was presented either in phase or out of phase with a counterphase flickering pedestal grating. These are the only experiments listed in Table 1 in which the pedestal was not static. They found normal threshold elevations (10% Weber fractions) for the in-phase condition, but minimal threshold elevation (or facilitation) for the quadrature condition. Although the test–pedestal phase-independence approach would not predict these results, these strong phase effects are not surprising for two reasons: (1) The test and the pedestal have identical Fourier spectra. In the in-phase condition the test adds with the same sign to both the rightward and the leftward Fourier components of the pedestal. In the out-of-phase condition the test adds with opposite signs to the two pedestal components. An opponent motion mechanism could easily detect the out-of-phase condition without being masked by the pedestal. (2) Klein and Tyler[35] showed how the strength of phase effects could be related to the stimulus autocorrelation function. Patterns with different second-order correlations (such as the pair of patterns used by Stromeyer *et al.*[32]) have different Fourier magnitudes and should be very discriminable. They would be expected to have different thresholds. Patterns 1–11 in Table 1 have identical second- and third-order correlations (to use the terminology of Klein and Tyler[35]) and should have similar detection thresholds and elevated discrimination thresholds. This principle explains the similar jitter and flicker detection thresholds as well as the slight elevation in discrimination thresholds compared with detection thresholds.

B. Facilitation and the Weber Fraction

On the right-hand side of Table 1 we have included a summary of test and pedestal interactions for each study listed in the table. In our jitter and flicker study (rows 1–3) we found a small amount of facilitation at low pedestal contrasts under some conditions. Wesemann and Norcia[10] seemed not to have found facilitation for jitter, however, they did not measure the low-contrast portion of the tvc curve, and they did not test detection thresholds without a pedestal. According to our findings their data would have revealed some facilitation if low pedestal contrasts had been investigated at the 10-Hz temporal frequency used in their study.

In the present study facilitation for jitter and flicker thresholds was greatest when the test temporal frequency was 5 Hz. A likely explanation for this selective facilitation is that, when the test temporal frequency is low and therefore similar to the stationary pedestal, the test and the pedestal will activate common mechanisms in the visual system. If the pedestal and the test are detected by different mechanisms, then the pedestal will have little or no effect on test stimulus detection, and therefore thresholds with and without the pedestal should be similar. This explanation agrees with data showing that facilitation is greatest when the test and the pedestal spatial characteristics are the same.[3,12,36] For conditions in which pedestal and test spatial and temporal frequencies are similar, the mechanism detecting the test would be able to interact with the pedestal and produce facilitation.[28] Stromeyer and Klein[28] found strong facilitation even when the test was at the third harmonic of the pedestal grating. It may be expected that the greatest facilitation would be found at the lowest temporal frequency (i.e., 2 Hz). The data shown in Fig. 9 appear to contradict this hypothesis, since greater facilitation is found at 5 Hz compared with 2 Hz. We were surprised by this result and do not have a good explanation for it.

Our peripheral data also show considerable facilitation for the jitter and the flicker detection tasks. It is likely that this facilitation is a case of uncertainty reduction by the pedestal. For stimulus detection at 17.5 deg in peripheral vision, the observer may not be certain about where to attend in their periphery. When a suprathreshold pedestal stimulus is also present, however, location uncertainty would be reduced, leading to greater visibility of the low-spatial-frequency test stimulus and thereby exhibiting facilitation.

Our jitter and flicker data demonstrate a Weber-like region starting at approximately 10–20 ctu. This finding differs from the low-contrast masking (lcm in Table 1) effect seen for contrast discrimination[3] and for motion created by a single displacement,[1] where the masking begins at lower pedestal contrasts. This difference in the pedestal masking power may result from the greater overlap in the test and the pedestal spatiotemporal spectrum in the stationary and the single-displacement data, since a

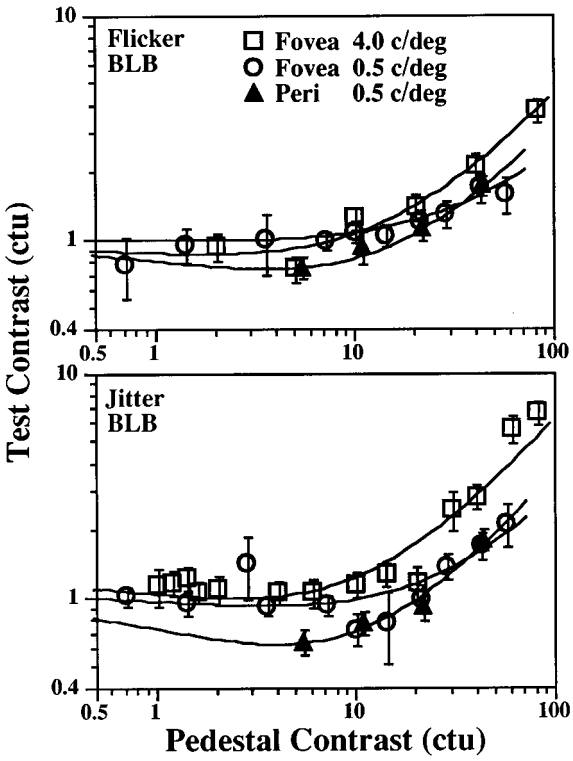

Fig. 15. Comparison of foveal 0.5-c/deg (○) and 4.0-c/deg (□) data with peripheral 0.5-c/deg (▲) data at a temporal frequency of 10 Hz. Flicker thresholds are shown in the upper panel; jitter, in the bottom panel.

single displacement has significant low-temporal-frequency energy. The importance of the test–pedestal temporal characteristics is seen in our study, where, as the relative temporal frequency of the test and the pedestal increasingly differed, Weber fractions were reduced.

Wesemann and Norcia[10] found a reduction in the Weber fraction with increases in eccentricity (see our Fig. 14). Our data also show this eccentricity effect if we compare the 4.0-c/deg foveal data with the 0.5-c/deg peripheral data, using the same scaling factor. This comparison is shown in Fig. 15. We have extended their findings to show that a rightward shift of the tvc curve is slightly more pronounced for the jitter than for the flicker task. Perhaps the temporal tuning of peripheral mechanisms differs from that of foveal mechanisms. It is possible that at this lower spatial frequency the pedestal is effectively stabilized and thus tends to fade, decreasing its effectiveness. We hypothesize that we also would have found reduced masking at higher spatial frequencies in the fovea if the experiment had been done with stabilized patterns.

C. Are Jitter and Flicker Processed within a Common Class of Mechanism?

Yet another goal in this paper was to determine whether the temporal characteristics of common underlying mechanisms can explain both jitter and flicker data. The data provide evidence suggesting that jitter and flicker are processed in common mechanisms. First, jitter and flicker detection thresholds were similar over a range of spatial and temporal frequencies. However, although similar detection thresholds suggest a common mechanism, it is possible that different mechanisms with similar response characteristics are mediating the two tasks. Evidence for some degree of separateness is shown by a slight elevation of flicker thresholds in several cases. Evidence for a common mechanism hypothesis is especially strong for temporal frequencies above 10 Hz, where in foveal and peripheral vision discrimination thresholds were elevated by a factor of 2 relative to detection thresholds. That jitter and flicker could not be discriminated at their detection thresholds suggests that common mechanisms are mediating both tasks.

There are at least two potential models of flicker/jitter discrimination that may explain how human observers discriminate temporal contrast increments and decrements from oscillatory motion. One of these involves mechanisms that are selectively sensitive to the direction of motion. Another model involves mechanisms that are space–time separable (a product of a spatial and a temporal term). Separable mechanisms are selectively sensitive to the relative spatial phase relationships of the flicker and the jitter component stimuli. First the space–time separable mechanism model is explored.

1. Space–Time Separable Mechanisms

One candidate class of mechanism that may be responsible for jitter and flicker detection and discrimination thresholds is space–time separable mechanisms. Figure 16 shows a range of potential responses to the flicker and jitter stimuli. Panels (a) and (e) show the response of a mechanism to the static pedestal and oscillating test patterns, respectively. Both temporal responses are windowed by a Gaussian, as was done in our experiments. Spatial filters that are aligned with the peak of the pedestal grating will respond strongly to the pedestal throughout its duration, as shown in Fig. 16(a). This filter will also respond to the flickering test when the test is in spatial phase with the pedestal. Therefore a common filter would respond to both the static pedestal and the flickering test grating. Other filters will not be optimally positioned (or eye movements will shift the original filter away from its optimal position), and the response to the pedestal will decrease. Panels (b)–(d) show the range of responses to the flicker stimulus for mechanisms at different positions. Panel (d) would be for a mechanism in the optimal position, whereas panel (b) would be for a mechanism placed spatially out of phase with the stimulus. Panels (f)–(h) represent responses to the jitter stimulus. In this case there is a decoupling of the pedestal and test responses, since the mechanisms optimally tuned for the pedestal would be poorly placed for the oscillating test. It is the space–time separability of the mechanisms that guarantees this behavior.

Figure 17 shows the graphic representation of the entire population of responding mechanisms, where the oscillatory and the static components of the response are plotted against each other. The responses to the flicker stimulus, shown in Figs. 16(b)–(d), are indicated in the top panel of Fig. 17 by the letters (b)–(d). Thus, for the flicker stimulus, the resulting scattergram would have a positive slope (i.e., a correlated activity in the static and the oscillatory responses). Similarly, a plot of the re-

sponse characteristics under jitter stimulus conditions would show a negative correlation between the responses to the test and the pedestal, as shown in the bottom panel of Fig. 17. The population statistics would be evaluated at the decision stage for the task of discriminating flicker from jitter.

This model does a good job in predicting our main results: (1) A space–time separable mechanism might be expected to produce greater masking effects for the flicker than for the jitter stimulus. This can, for example, be seen in panel (h) of Fig. 16. For the jitter stimulus there will be mechanisms that respond well to the oscillating test but not to the static pedestal. These mechanisms might be expected to show no masking (or reduced masking) by the pedestal even at high pedestal contrasts. However, for the flicker stimulus, as shown in panel (d) (or in the left-hand panel of Fig. 17), the mechanism that has the greatest sensitivity to the test would also be most masked by the pedestal. We found, though, that masking was only slightly greater for flicker than for jitter. This near equality of the jitter and the flicker data may be explained by a contrast gain control stage in which the gain control pool combines the output from all the phase-specific detectors. A saturating energy model[27] would produce the same effect. (2) This model could predict the temporal dependence of the masking effect where low temporal frequencies showed greater masking for the flicker stimulus, especially in the periphery (see Fig. 13). The somewhat greater masking for flicker could come from a response saturation, since the detection mechanism is now responding to the mask as well as the test. The near equality of jitter and flicker detection thresholds at higher temporal frequencies could be achieved by the temporal tuning of the mechanisms where, at high temporal frequencies, the pedestal response is diminished. (3) The separable mechanism model is also compatible with the discrimination performance. Figures 12 and 13 show that, at the lower temporal frequencies, discrimination is almost as good as detection. At higher temporal frequencies discrimination is reduced by a factor of 2–3. Good performance would imply that the decision stage is capable of extracting the information available in the population statistics of Fig. 17. At higher temporal frequencies the mechanisms responding to the test have reduced response to the pedestal, evidenced by the reduced Weber fractions shown in Figs. 9 and 10. This would result in a compression of the horizontal axis in Fig. 17, thus making the discrimination judgment more difficult. Compression of the horizontal axis is also effectively achieved by use of low pedestal contrasts. However, in that case discrimination was found to be good, as shown in Figs. 7 and 8, so another explanation is needed.

The discrimination could then be done by comparison of the spatial locations of the mechanisms responding to the test and the mechanisms responding to the pedestal. If aligned, the pattern would be judged to be flicker, and, if offset, it would be judged to be jitter. An argument

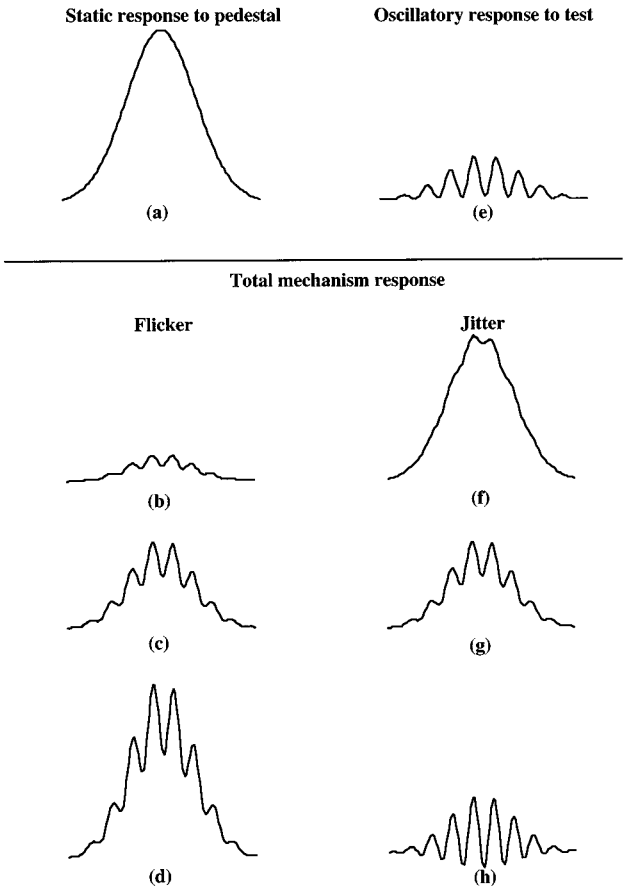

Fig. 16. Schematic of a separable model of flicker/jitter discrimination. (a), (e) Temporal response of a mechanism to static pedestal and oscillatory test gratings, respectively. (b)–(d), (f)–(h) Combined responses to the flicker and the jitter stimuli, respectively, at different points in time.

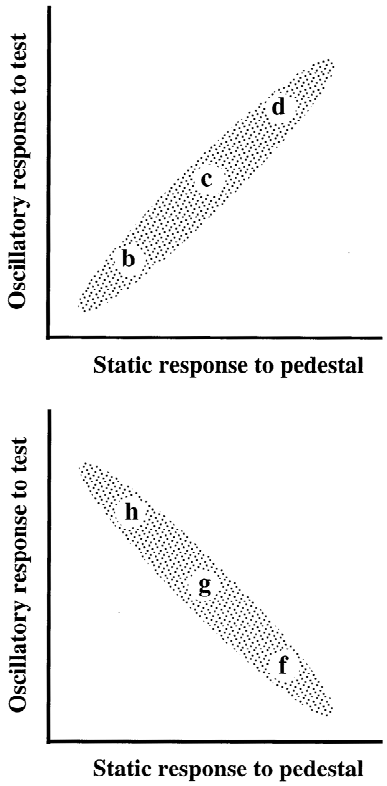

Fig. 17. Plot of the separable mechanism responses in time (as described in Fig. 16).

against this possibility is data collected on SAK (not shown in Fig. 12) by use of 20-c/deg gratings with a 5-Hz counterphase test. The contrast thresholds were 11.7%, 11.0%, and 10.4% for flicker, jitter, and discrimination, respectively. At 20 c/deg, the relative phase shift between pedestal and test is 3/4 arcmin. It is amazing that the phase could be assessed that accurately.

2. Motion Mechanisms

An alternative candidate mechanism that may account for our data on detection and discrimination thresholds for jitter and flicker is a direction-selective filter. This filter is assumed to respond to the pedestal and to only one of the motion directions of the counterphase test pattern because of its directional selectivity. To clarify how these motion mechanisms respond to the test patterns, Fig. 18 presents how the stimulus would appear when filtered through one of these motion mechanisms. The horizontal and the vertical axes represent position and time, respectively. The vertical bands represent the stationary pedestal, and the diagonal bands represent one of the moving components of the counterphase test pattern. The band tilted to the right is the moving sinusoid seen by rightward-selective mechanisms. In our experiments the motions were up and down, but in Fig. 18 we depict them as right and left for clarity. The points at which the test and the pedestal are in phase are the points at which the mechanisms are optimally stimulated. These space–time regions are shown in black. For the flicker task, symmetry implies that the peak stimulation occurs at the same time for the rightward and the leftward mechanisms. This is shown in Fig. 18 by the black diamonds that occur simultaneously. For the jitter task, however, there is an asymmetry between the rightward and the leftward mechanisms. The 90-deg advance and retardation of the rightward and the leftward stimulus components, respectively, results in a 180-deg shift of the peak activation of the two components. The 90-deg shift occurs because the pedestal is shifted spatially by 90 deg in the jitter stimulus compared with the flicker stimulus. A 90-deg leftward phase shift of the pedestal produces a delayed 90-deg temporal phase shift in timing of when the peak of the leftward-moving grating coincides with the pedestal peak. Similarly, there would be a phase advance for the rightward component peak coinciding with the pedestal peak. That is, for flicker the rightward and the leftward mechanisms would respond in phase with each other, whereas for jitter they would be 180 deg out of phase with each other. At a second comparison stage, this temporal response phase difference could be used for discriminating between jitter and flicker.

This motion model can explain a number of our results: (1) The near equality of jitter and flicker detection thresholds is explained because any single mechanism responds identically to both flicker and jitter. (2) The direction-selective filters would predict our jitter-versus-flicker discrimination results, since at low temporal frequencies the temporal discrimination depicted in Fig. 18 should easily be achieved. At high temporal frequencies the temporal phase discrimination becomes more difficult (because of the relative temporal phase judgment), accounting for the falloff shown in Fig. 12. At low temporal frequencies discrimination was possible at the detection threshold. SAK's good discrimination at 20 c/deg, mentioned above, could also be explained by this model, since accurate spatial localization is not required.

The motion mechanism model does not easily explain the slightly lower detection thresholds for jitter as opposed to flicker. A composite model in which a local gain control, with some phase selectivity, followed by a motion-selective mechanism, should be able to predict the data. Figure 12 shows that the lack of detection equality is found mainly below 5 Hz, which suggests that the local gain control has a low-pass behavior.

One might think that there is ample past evidence favoring unidirectional motion mechanisms over the separable mechanisms. For example, Levinson and Sekuler[14] compared the visibility of a moving sinusoidal grating with the visibility of a counterphase grating of the same spatial and temporal frequencies. They explained the 2:1 ratio of visibility in terms of underlying direction-selective motion mechanisms. But this 2:1 ratio of visibility is limited to the regime in which the velocities are large.[18] At low velocities (low hertz) that ratio no longer holds. Non-direction-selective mechanisms (spatial phase-selective mechanisms) might be dominant in that regime. Furthermore, studies that were done without a

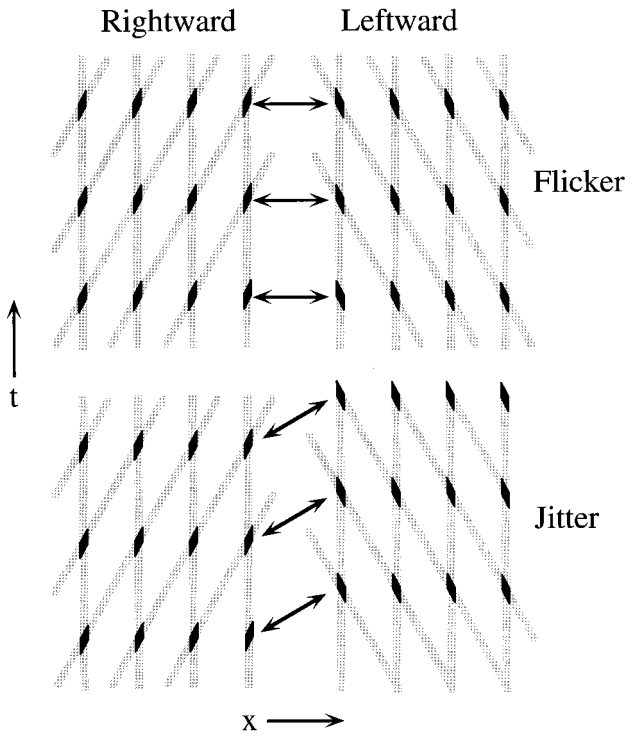

Fig. 18. Schematic of a motion model of flicker/jitter discrimination. The horizontal and the vertical directions correspond to space and time, respectively. The vertically oriented bars are the pedestal grating peak locations. The left-hand pair of panels represent the stimuli as seen by rightward motion mechanisms. The right-hand pair of panels represent the stimuli as seen by leftward motion mechanisms. The diagonal bars are the peaks of the rightward and the leftward components of the counterphase test grating as seen by their respective motion mechanisms. The arrows show that, for the flicker stimulus, the peak activity of the rightward and the leftward mechanisms is simultaneous and that, for the jitter stimulus, their peak activity has a relative 180-deg temporal phase shift.

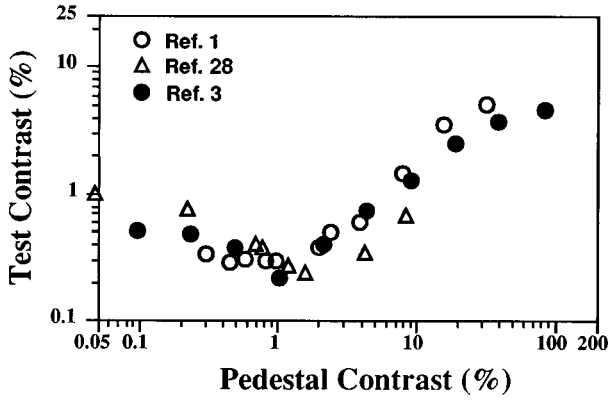

Fig. 19. Three data sets are shown. The first is a replot (○) of converted scores from the Nakayama–Silverman[1] motion displacement study. Another data set is a replot (●) of Fig. 1 (observer JMF) from the static contrast discrimination data in Legge and Foley.[3] Also shown (△) are converted scores of static contrast discrimination data found in Stromeyer and Klein.[28]

visible static pedestal might not be relevant to experiments in which a strong pedestal is present. The contrast gain control could change the operating characteristics of the underlying mechanisms.

D. Saturating Filters: Hard Saturation

Our sixth goal was to compare our jitter results with the single-displacement results obtained by Nakayama and Silverman.[1] Do motion mechanisms saturate? Here we provide support for the notion that motion channels may not show low-contrast saturation but instead may have a contrast gain control mechanism, or noise, that increases with pedestal contrast.

Nakayama and Silverman[1] suggested that contrast processing of the motion system is distinct from contrast discrimination because there is a strong contrast saturation of single-displacement motion thresholds starting at low contrasts. They plotted single-displacement data in terms of phase angle as a function of contrast. Phase angle thresholds decreased with increases in contrast for contrasts below approximately 2% and become constant for contrasts above approximately 2%. They stated that their single-displacement data differed from classical contrast discrimination studies,[2,3,28] since those studies find weaker (logarithmic) contrast saturation up to pedestal contrasts of 100%.

We have shown that oscillating motion and contrast flicker are likely mediated within common mechanisms. But are other forms of motion, such as abrupt displacements, and contrast discrimination processed in common mechanisms? Following the test–pedestal approach, we would predict similar thresholds for the discrimination of single displacements and the detection of a contrast increment, since the test and the pedestal gratings are the same for both stimuli, differing only in their phase relationship. The contrast discrimination tvc function, including our flicker detection data, is thought to reflect a contrast gain control mechanism. This possibility was noted but not explored in Nakayama and Silverman[1] (p. 272). We transformed the Nakayama–Silverman[1] phase angle thresholds to test contrast thresholds, using $c_t = c_p \sin(\phi)$, where ϕ is the direction discrimination phase threshold. The open circles in Fig. 19 show the resulting tvc plot for the Nakayama–Silverman[1] observer JS. Also shown are classical tvc curves obtained with stationary gratings replotted from Fig. 2 of the Legge–Foley[3] study (observer JMF) and from Fig. 3 of the Stromeyer–Klein[28] study. The three curves in Fig. 19 are very similar. Differences shown may result from experimental procedure and individual observer differences. This point was made earlier by Klein and Levi[27] in their Appendix 4. In their Fig. 10d, they show both the tvc curve and the Nakayama–Silverman[1] effective contrast plot.

In conclusion, the implication of the transformed Nakayama–Silverman[1] phase angle thresholds to test contrast thresholds is that the widely held assumption that motion saturates at low contrasts may not be valid. The saturating behavior reported by Nakayama and Silverman[1] does not necessarily demonstrate saturation of the underlying mechanism. We suggest that, like contrast processing, the motion system is sensitive to abrupt displacements and exhibits behavior consistent with a single underlying contrast gain control mechanism common to both motion and contrast.

APPENDIX A: THREE TYPES OF TEST–PEDESTAL EXPERIMENTS FOR OFFSET DETECTION AND DISCRIMINATION

Many of the experiments discussed in this paper use a sinusoidal test grating added to a pedestal to produce a grating shifted by some phase angle ϕ. Our goal in this appendix is to clarify the relation between the angle ϕ and the test and pedestal contrasts. We also hope to clarify subtle differences between detection and discrimination that can lead to confusion.

1. Case 1: Test Added in Quadrature to Pedestal

The stimulus used in the present experiments for the detection of jitter is

$$c_p \cos(fx) + c_t \sin(fx)\sin(\omega t), \tag{A1}$$

where c_p and c_t are the pedestal and the test contrasts, respectively. The observer's task is to discriminate between the jittering grating given by expression (A1) and the static pedestal, $c_p \cos(fx)$. The first row of Fig. 20 is the stimulus at those instants when the phase shift is maximum [$\sin(\omega t) = 1$]. This case differs from the other three cases (see Fig. 20) discussed below, in that the instantaneous contrast is not constant. The maximum contrast is given by the Pythagorean sum of c_p and c_t:

$$c_{p+t} = (c_p{}^2 + c_t{}^2)^{0.5} = c_p/\cos(\phi). \tag{A2}$$

Figure 20 (case 1) also presents a graphical representation, or phasor diagram, of the interrelationship of these quantities. The pedestal (with zero phase shift) is along the horizontal axis, and the test (with 90-deg phase shift) is along the vertical axis. The test plus pedestal stimulus is along the hypotenuse, c_{p+t}.

	Interval 1	Interval 2	Test Pattern	for c_{ti} defined as	Phasor diagrams
Case 1	$c_p \cos(fx)$	$(c_p^2 + c_t^2)^{0.5}\cos(fx+\phi)$	$c_{t1} \sin(fx)$	$c_{t1} = c_p \tan(\phi)$	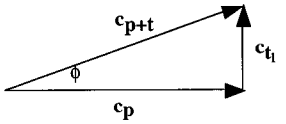
Case 2a	$c_p \cos(fx)$	$c_p \cos(fx+\phi)$	$c_{t2} \sin(fx+\phi/2)$	$c_{t2} = c_p\, 2 \sin(\phi/2)$	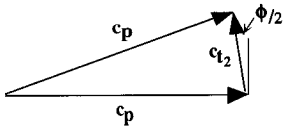
Case 2b	$c_p \cos(fx - \phi/2)$	$c_p \cos(fx + \phi/2)$	$c_{t2} \sin(fx)$	$c_{t2} = c_p\, 2 \sin(\phi/2)$	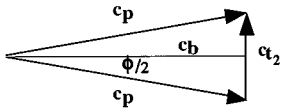
Case 3	$c_p \cos(fx)$	$c_p \cos(fx+\phi)$	$\pm c_{t3} \sin(fx)$	$c_{t3} = c_p \sin(\phi)$	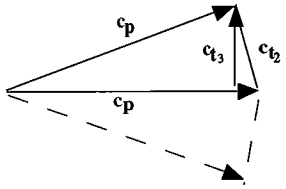

Fig. 20. Distinction of four test–pedestal relationships. Phasor plots are shown for each test (c_t) and pedestal (c_p) stimulus.

2. Case 2: Detection of a Jump

Nakayama and Silverman[1] and Levi *et al.*[25] carried out two types of experiments with single displacements of a grating: detection and discrimination of motion. In the detection task one must discriminate between a stationary grating (the blank) given by $c_p \cos(fx)$ and a grating that abruptly moves or jumps, given by $c_p \cos(fx + \phi)$. The second row of Fig. 20 presents this stimulus. The third column of Fig. 20 gives the test signal, $c_{t2} \sin(fx + \phi/2)$, which is the difference between the two stimuli being discriminated. The phasor diagram of the situation corresponding to the phases is also shown. Notice that this test signal has an extra phase of $\phi/2$ as compared with the other two cases. This phase could have been eliminated if the origin of the x axis were defined such that the initial image was $c_p \cos(fx - \phi/2)$. The jumped image would then be $c_p \cos(fx + \phi/2)$. In that case, the test pattern becomes $c_t \sin(fx)$, similar to case 1. The phasor diagram corresponding to the situation just discussed is shown in Fig. 20 (case 2b).

Figure 20 also presents the case 2 stimulus in this second way (third diagram from top). One can think of the stimulus as consisting of a static background component given by $c_b \cos(fx)$ plus a test component given by $c_t \sin(fx)R(t)$, where $c_b = [c_p{}^2 - (c_t/2)^2]^{0.5}$ and where $R(t)$ is given by Eq. (3) as $+0.5$ for $t > 0$ and -0.5 for $t < 0$. This method of writing the stimulus has the advantage, shown in Fig. 20, that the static components are pure cosine and the test components are pure sine. The disadvantage is that the static component does not have the full pedestal contrast.

The same analysis can be applied to vernier acuity. The only change needed is to replace t with y. In Table 1, $R(t)$ is replaced by $R(y)$ for the case of vernier acuity. A vernier detection task involves discriminating a vernier offset from zero offset.[37] A vernier discrimination task (case 3) involves discriminating a rightward offset from a leftward offset.

The distinction between cases 1 and 2 can be subtle. Both involve the detection of an offset. The difference has to do with how the pedestal contrast is defined. Let us write the stimulus as $c_b \cos(fx) + c_t R(t)\sin(fx)$, where c_b is the background contrast. In the present study the reversal function, $R(t)$, was $\cos(\omega t)$, and in the Wesemann–Norcia[10] study it was a square wave going between levels ± 0.5. In our study the background stimulus was the pedestal (i.e., $c_p = c_b$). As the test contrast became larger, the maximum contrast of test plus pedestal also became larger [see Eq. (A2)]. In their study, Wesemann and Norcia produced the stimulus by jumping the grating back and forth rather than by adding a test to a pedestal. The background term $c_b \cos(fx)$ was never seen. We have thus come to the interesting conclusion that, simply by changing the stimulus from sinusoidal oscillation to square-wave oscillation, we have changed from a case 1 stimulus to a case 2 stimulus. When comparing test thresholds in these two cases it must be kept in mind that for case 1 the displacement phase is from

midpoint to maximum, while in case 2 it is from minimum to maximum. For case 1 the test contrast is given by $c_p \tan(\phi)$, and in case 2 it is $2c_p \sin(\phi/2)$. Luckily, as shown in Fig. 21, these two definitions are almost indistinguishable for displacements less than approximately 20 deg. Only at low pedestal contrasts are the displacement thresholds larger than 20 deg.

3. Case 3: Direction Discrimination of a Jump

In their second type of experiment Nakayama and Silverman[1] and Levi *et al.*[25] discriminated the direction of motion. The task was to discriminate between a grating that jumped to the right or to the left. This is different from the stimulus discussed in cases 1 and 2, since the observer not only must detect the jump but also must identify its direction. The test pattern from case 2 can be written as

$$\begin{aligned} T_{\text{tot}}(x) &= c_p[\cos(fx + \phi) - \cos(fx)] \\ &= c_p\{\cos(fx)[\cos(\phi) - 1] - \sin(fx)\sin(\phi)\}. \end{aligned} \tag{A3}$$

This decomposition of the test pattern into two terms is the same decomposition into the bipolar and monopolar terms discussed by Klein.[24] The bipolar term [proportional to $\sin(fx)$] switches sign for rightward and leftward jumps ($+\phi$ and $-\phi$). The monopolar term [proportional to $\cos(fx)$] has the same sign for both rightward and leftward jumps. Thus only the bipolar term contributes to the direction discrimination, and the test pattern for the discrimination task is

$$T_{\text{disc}} = c_t \sin(fx), \tag{A4}$$

where

$$c_t = c_p \sin(\phi). \tag{A5}$$

This last result could be derived from the phasor diagram shown in case 3 of Fig. 20.

The easiest way to distinguish between the detectability of motion (did it move?) and the discriminability of motion (in which direction did it move?) is to carry out separate experiments, as was done by Nakayama and Silverman.[1] The detection task would be to discriminate stationary from rightward jumps, and the discrimination task would be to discriminate leftward from rightward jumps. One can also measure both detection and discrimination in the same experiment.[24,25] The experiments of Levi *et al.*[25] are relevant to the present discussion since they involved the detection and direction discrimination of a displacement of a grating. Reference 25 is similar to the Nakayama–Silverman[1] experiment except that, instead of a sinusoidal grating, a rectangular grating made of thin white lines was used at a wide range of spatial frequencies. At the higher spatial frequencies a rectangular grating becomes very similar to a sinusoidal grating. Levi *et al.*[25] found that in foveal vision of normal observers the thresholds for detection and discrimination of displacement are similar. However, in peripheral vision (and in foveal vision of strabismic amblyopes) detection thresholds were lower than discrimination thresholds. They also found that there were marked differences in threshold depending on whether a reference was present.

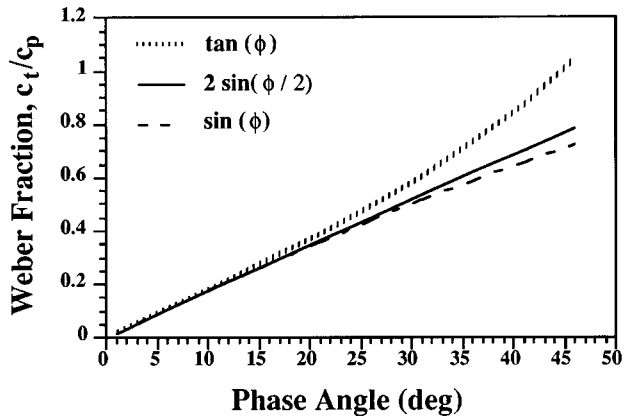

Fig. 21. Weber fraction, c_t/c_p, shown as a function of phase angle for the three cases described in Fig. 20. The Weber fractions are similar for phase angles of less than 20 deg.

Case 3 also applies to vernier acuity, where the displacement is in space rather than in time. As an example of how easy it is to confuse cases 2 and 3, consider the paper of Hu *et al.*,[4] who inadvertently confused case 3 with case 2a. Their experiment used the method of constant stimuli to present vernier stimuli with a range of offsets (negative, zero, and positive). The observer gave rating-scale responses about the direction and the magnitude of the perceived offset. The analysis that was performed on the data was appropriate for a discrimination task in which rightward offsets are distinguished from leftward offsets. This seems to be a clear case 3 experiment. In the mathematical description of the stimulus, however, Hu *et al.*[4] treated the stimulus as if it were a case 2a detection task. This confusion had minimal consequences on their results, since the vernier offsets involved small phase angles where there is little difference among the three cases, as shown in Fig. 20. The fourth column of Fig. 20 shows that the Weber fraction c_t/c_p can be related to the phase jump in three manners: $\tan(\phi)$, $2\sin(\phi/2)$, and $\sin(\phi)$ for cases 1, 2, and 3, respectively. Figure 21 presents plots of these three trigonometric functions. For phase angles less than approximately 20 deg, there is very little difference among the different test stimulus definitions. The error made by Hu *et al.*[4] points out how easy it is to confuse the three cases.

APPENDIX B

Our seventh goal in this project was to develop a novel contrast discrimination dipper function fit for conditions in which the test and the pedestal stimuli are not the same. We fitted the raw (nonnormalized) threshold data with a tvc curve derived from the transducer function discussed by Klein and Levi[27]:

$$d'(c) = \ln[1 + nw(c/T)^n]/\ln(1 + nw), \tag{B1}$$

where c is the effective contrast [see Eq. (B5)], T is the contrast at which d' is unity, and n is the transducer ex-

ponent that controls the low-contrast power function behavior of the transducer function.

Equation (B1) is a three-parameter fit to the dipper function. We have modified the original equation of Klein and Levi,[27] replacing their $1/W$ with nw. This changes the definition of w, as shown in the following equations, so that it represents the high-contrast Weber fraction.

For our present application, we slightly modified Eq. (B1) because the pedestal and the test stimuli have different temporal frequencies, thus affecting the detection mechanisms differently. We include this effect in the contrast term of Eq. (B1) by summing the test and the pedestal contrasts normalized by their thresholds:

$$c/T = c_t/T_t + c_p/T_p, \tag{B2}$$

where c_t is the test contrast, c_p is the pedestal contrast, T_t is an estimate of the test detection threshold, and T_p is the static pedestal detection threshold estimate.

To use the transducer function of Eq. (B1) to fit the data in the fashion shown in Figs. 5–8, the threshold condition is written as

$$d'(c_p/T_p + c_t/T_t) - d'(c_p/T_p) = 1. \tag{B3}$$

By solving Eq. (B3) for c_t, one obtains the magnitude of test contrast that is needed to increase d' by unity. Although Eq. (B3) in combination with Eq. (B1) looks like a complicated nonlinear equation, Klein and Levi[27] showed that it has a simple analytic exact solution:

$$c_t = \{[1 + (c_p/T_p)^n(1 + nw)]^{1/n} - c_p/T_p\}T_t. \tag{B4}$$

For large c_p this becomes

$$c_t/T_t \approx c_p/T_p[(1 + nw)^{1/n} - 1]. \tag{B5}$$

For small values of w (as is always the case for our data), Eq. (B4) becomes

$$c_t/T_t = w(c_p/T_p). \tag{B6}$$

The parameter w is the Weber fraction relating test contrast (in ctu) to pedestal contrast (also in ctu).

Typical tvc curves (where the test and the pedestal are the same stimulus) would have c_t increasing as $c_p{}^{0.7}$ at large c_p rather than the linear increase given by Eq. (B6). This property could have been included in our model by replacement of the logarithm by a power function with an exponent of -0.3. However, the fit with the simpler logarithm was adequate for the present purposes.

ACKNOWLEDGMENTS

This research was supported by the National Eye Institute (grant EY0-4776) and by the U.S. Air Force Office of Scientific Research (grant F49620-95-C-0018). Preliminary data were presented at the 1994 Association for Research in Vision and Ophthalmology meeting in Sarasota, Florida.

REFERENCES AND NOTES

1. K. Nakayama and G. H. Silverman, "Detection and discrimination of sinusoidal grating displacements," J. Opt. Soc. Am. A **2**, 267–274 (1985).
2. J. Nachmias and R. V. Sansbury, "Grating contrast: discrimination may be better than detection," Vision Res. **14**, 1039–1042 (1974).
3. G. E. Legge and J. M. Foley, "Contrast masking in human vision," J. Opt. Soc. Am. **70**, 1458–1471 (1980).
4. Q. Hu, S. A. Klein, and T. Carney, "Can sinusoidal vernier acuity be predicted by contrast discrimination?" Vision Res. **33**, 1241–1258 (1993).
5. S. A. Klein, E. Casson, and T. Carney, "Vernier acuity as line and dipole detection," Vision Res. **30**, 1703–1719 (1990).
6. H. R. Wilson, "Responses of spatial mechanisms can explain hyperacuity," Vision Res. **26**, 453–469 (1986).
7. D. L. Levi, S. A. Klein, and H. Wang, "Amblyopic and peripheral vernier acuity: a test–pedestal approach," Vision Res. **34**, 3265–3292 (1994).
8. D. L. Levi, S. A. Klein, and H. Wang, "Discrimination of position and contrast in amblyopic and peripheral vision," Vision Res. **34**, 3293–3313 (1994).
9. T. Carney and S. A. Klein, "Resolution is better than vernier acuity," Vision Res. **37**, 525–540 (1997).
10. W. Wesemann and A. M. Norcia, "Contrast dependence of the oscillatory motion threshold across the visual field," J. Opt. Soc. Am. A **9**, 1663–1671 (1992).
11. M. J. Wright and A. Johnston, "The relationship of displacement thresholds for oscillating gratings to cortical magnification, spatiotemporal frequency and contrast," Vision Res. **25**, 187–193 (1985).
12. I. BodisWollner and C. D. Hendley, "On the separability of two mechanisms involved in the detection of grating patterns in humans," J. Physiol. (London) **291**, 251–263 (1979).
13. T. B. Lawton and C. W. Tyler, "On the role of *X* and simple cells in human contrast processing," Vision Res. **34**, 659–667 (1994).
14. E. Levinson and R. Sekuler, "The independence of channels in human vision selective for direction of movement," J. Physiol. (London) **250**, 247–266 (1975).
15. A. B. Watson, P. G. Thompson, B. J. Murphy, and J. Nachmias, "Summation and discrimination of gratings moving in opposite directions," Vision Res. **20**, 341–347 (1980).
16. M. Green, "Psychophysical relationships among mechanisms sensitive to pattern, motion and flicker," Vision Res. **21**, 971–983 (1981).
17. P. Thompson, "Discrimination of moving gratings at and above detection threshold," Vision Res. **23**, 1533–1538 (1983).
18. C. F. Stromeyer III, J. C. Madsen, S. A. Klein, and Y. Y. Zeevi, "Movement-selective mechanisms in human vision sensitive to high spatial frequencies," J. Opt. Soc. Am. **68**, 1002–1005 (1978).
19. A. T. Smith, "Velocity perception and discrimination: relation to temporal mechanisms," Vision Res. **27**, 1491–1500 (1987).
20. A. B. Watson and J. G. Robson, "Discrimination at threshold: labeled detectors in human vision," Vision Res. **21**, 1115–1122 (1981).
21. J. Rovamo and V. Virsu, "An estimation and application of the human cortical magnification factor," Brain Res. **37**, 495–510 (1979).
22. D. L. Levi, S. A. Klein, and P. Aitsebaomo, "Vernier acuity, crowding and cortical magnification," Vision Res. **25**, 963–977 (1985).
23. Appendix A describes similarities and differences in three possible test–pedestal relationships in which the test is shifted by some phase angle. Case 1 in Appendix A describes the jitter stimulus used in the current experiments.
24. S. A. Klein, "Double-judgment psychophysics: problems and solutions," J. Opt. Soc. Am. A **2**, 1560–1585 (1985).
25. D. L. Levi, S. A. Klein, and P. Aitsebaomo, "Detection and

discrimination of the direction of motion in central and peripheral vision of normal and amblyopic observers," Vision Res. **24**, 789–800 (1984).
26. S. A. Klein, "An EXCEL macro for transformed and weighted averaging," Behav. Res. Methods Instrum. Comput. **24**, 90–96 (1992).
27. S. A. Klein and D. L. Levi, "Hyperacuity thresholds of one second: theoretical predictions and empirical validation," J. Opt. Soc. Am. A **2**, 1170–1190 (1985).
28. C. F. Stromeyer III and S. A. Klein, "Spatial frequency channels in human vision as asymmetric (edge) mechanisms," Vision Res. **14**, 1409–1420 (1974).
29. A. Bradley and B. Skottun, "Effects of contrast and spatial frequency on vernier acuity," Vision Res. **27**, 1817–1824 (1987).
30. J. P. Harris and M. Fahle, "The detection and discrimination of spatial offsets," Vision Res. **35**, 51–58 (1995).
31. J. H. T. Jamar, L. F. T. Kwakman, and J. J. Koenderink, "The sensitivity of the peripheral visual system to amplitude-modulation and frequency-modulation of sine-wave patterns," Vision Res. **24**, 243–249 (1984).
32. C. F. Stromeyer III, R. E. Kronauer, J. C. Madsen, and S. A. Klein, "Opponent-movement mechanisms in human vision," J. Opt. Soc. Am. A **1**, 876–884 (1984).
33. J. Lubin, "Interactions among motion-sensitive mechanisms in human vision," Ph.D. dissertation (University of Pennsylvania, Philadelphia, Pa., 1992).
34. Before continuing this discussion of studies within a test–pedestal framework, we should differentiate two types of discrimination tasks. In the discrimination task used in the present study, jitter and flicker represent independent dimensions; they involve two-knob experiments, to use the nomenclature of Klein.[24] This type of discrimination can be distinguished from a vernier discrimination task, in which an observer is asked to discriminate the direction of the vernier offset (rightward versus leftward) along a continuum, referred to as a single-knob experiment.[24] Based on these definitions, the Nakayama–Silverman[1] displacement discrimination was a single-knob experiment. In a single-knob experiment the discrimination d' tends to be double the detection d'. For double-knob experiments with independent, labeled detectors, the discrimination d' can be as high as $\sqrt{2}$ times the detection d'.[24]
35. S. A. Klein and C. W. Tyler, "Phase discrimination of compound gratings: generalized autocorrelation analysis," J. Opt. Soc. Am. A **3**, 868–879 (1986).
36. A. J. Pantle, "Temporal determinants of spatial sine-wave masking," Vision Res. **23**, 749–757 (1983).
37. Y. L. Yap, D. M. Levi, and S. A. Klein, "Peripheral hyperacuity: three-dot bisection scales to a single factor from 0 to 10 degrees," J. Opt. Soc. Am. A **4**, 1554–1561 (1987).